NASA TN D-1491

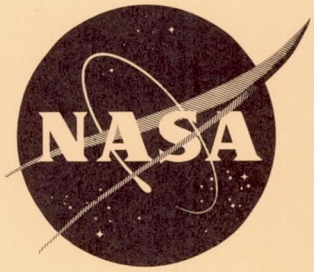

TECHNICAL NOTE

D-1491

TRANSITION AND HOVERING FLIGHT CHARACTERISTICS OF A TILT-DUCT VTOL RESEARCH AIRCRAFT

By Henry L. Kelley

Langley Research Center
Langley Station, Hampton, Va.

NATIONAL AERONAUTICS AND SPACE ADMINISTRATION
WASHINGTON
November 1962

NATIONAL AERONAUTICS AND SPACE ADMINISTRATION

TECHNICAL NOTE D-1491

TRANSITION AND HOVERING FLIGHT CHARACTERISTICS OF A TILT-DUCT VTOL RESEARCH AIRCRAFT

By Henry L. Kelley

SUMMARY

Flight measurements of various aerodynamic characteristics of a tilting ducted-fan, vertical-take-off-and-landing (VTOL) research aircraft have been recorded over the transition speed range during testing at the Langley Research Center and are presented in conjunction with pilots' observations. Test results cover a speed range of 35 knots to 115 knots and duct angles from 60° to 0°.

Stalling of outer wing surfaces limited the rate of descent capabilities of the tilt-duct aircraft in the transition speed range. One possible method of reducing the adverse stall effects in the steady-state descent condition consisted in holding a constant angle of attack well below wing stall by raising the duct angle and dropping the nose below the horizontal.

Static stability investigations (apparent directional stability and effective dihedral) indicated stability of varying degree throughout the range investigated, and pilots reported that the static stability went from marginally satisfactory at the high-speed end of the transition speed range to unsatisfactory at the low-speed end. Longitudinal and lateral-directional oscillations were well damped over the portion of the transition speed range investigated. Pilots' comments indicated that the damping of all oscillations studied was satisfactory.

A limited hovering investigation indicated undesirably low control power and angular-velocity damping about the roll and yaw axes, which tends to confirm the necessity for this type of aircraft to meet minimum helicopter requirements. Motion of the aircraft about the pitch axis was controllable and was considered acceptable for research flying and, according to pilots' comments, would probably meet minimum helicopter requirements. Static rig measurements of the tilt-duct configuration indicated that downwash from the ducted fans being reflected from the ground contributed in part, at least, to uncontrollable lateral destabilizing tendencies experienced during hovering flight.

INTRODUCTION

The National Aeronautics and Space Administration has been active in VTOL (vertical take-off and landing) research programs, utilizing VTOL test-bed aircraft, for the past several years. These research programs have been conducted

to establish design criteria and operational procedures for general application to the entire spectrum of VTOL aircraft configurations.

Reference 1 presents early flight test results from a tilting ducted-fan VTOL research vehicle. Similar flight testing was conducted on a tilt-wing VTOL research aircraft and the results are presented in references 2 and 3. Additional results from a wind-tunnel investigation on a ducted-fan configuration are presented in references 4 and 5.

This paper presents the results of a more extensive flight investigation with the tilt-duct aircraft than was presented in reference 1. The purpose of the tests was to provide data from which general conclusions could be drawn that would apply to any similar tilt-duct configuration. The portion of the transition speed range investigated was 35 knots to 115 knots. A qualitative study of the hovering flight characteristics was also made.

SYMBOLS

P	engine shaft horsepower, hp
V	indicated airspeed along flight path, knots
α_f	fuselage angle of attack with respect to free stream, deg
α_w	wing angle of attack, $\alpha_f + 2.5^\circ$, deg
β	sideslip angle, deg
δ_d	duct deflection relative to wing chord line, deg

APPARATUS AND PROCEDURE

Aircraft

The tilt-duct vertical-take-off-and-landing configuration is shown in figures 1 and 2. This aircraft is similar in configuration to a conventional airplane except that a tilting ducted-fan assembly is mounted at each wing tip to provide propulsion and VTOL capability. The thrust axis of these ducted fans can be rotated from a position perpendicular to the wing chord plane for hovering flight to a position essentially parallel to the wing chord for conventional airplane flight. The principal physical dimensions of this aircraft are listed in table I. A more complete description of the ducted fan is included in reference 4.

Control Systems

Reference 1 presents a general description of the control systems in the hovering, transition, and forward-flight configuration. Table II presents dimensions and characteristics of the control surfaces.

Pitch trim flaps (fig. 1) have been added to the exit of each duct to help reduce the nose-up pitching moments, which were discussed in reference 1. These pitch trim flaps were programed with the angle of duct rotation by a cam arrangement to give a greater nose-down moment at the higher duct angles (lower speeds) where control margins were a minimum. Before the present flights were undertaken, the cam was modified to increase the nose-down moment. The programed deflection of the flaps with duct angle obtained with the modified cam is shown in figure 3 and is compared with that obtained with the original cam design.

The horizontal stabilizer, as was mentioned in reference 1, can be varied through 10° to aid in trimming the aircraft longitudinally in the transition region when the ducts are set for transition airspeeds. This control must be operated manually by the pilot during the transition. No automatic stabilization equipment was included in the control system.

Test Conditions and Procedures

Flight tests.- Data taken during flight testing of the tilt-duct research aircraft included level-flight data, steady-state rates of descent, rates of climb, longitudinal and lateral-directional oscillations, and sideslips. Qualitative investigations were also made in the hovering flight region. All test flights were made in relatively calm air (a wind velocity of 10 knots or less).

Flight techniques used during descents and for stalling investigations involved two methods. One method involved varying the power and holding the angle of attack constant, letting the airspeed vary accordingly. The second method involved varying the power and holding a constant airspeed, allowing the angle of attack to vary accordingly. Data showing aircraft dynamic and static characteristics were obtained using standard flight test techniques. Only limited hovering flight tests were made - owing, in part, to the lateral destabilizing tendencies resulting from the flow field in the presence of the ground.

Static tests.- A static test rig was designed and built to provide simulated hovering flight at three positions above the ground. The positions selected were 4, 6, and 8 feet measured from the ground to the trailing edge of the duct. At each position the aircraft was banked at angles which varied from 10° right to 10° left. The power was set at 80 percent of engine gas producer speed at each test condition and represented about 350 shaft horsepower (41 percent of the hovering shaft horsepower).

Instrumentation

Flight test.- The airspeed, pressure altitude, angle of attack, duct angle, engine-output shaft speed, horizontal-stabilizer angle, and engine gear-box oil

pressure (provides torque output reference) are recorded by two motion-picture cameras photographing the pilot's instrument panel. The duct forces and moments are sensed by strain-gage bridges mounted on the duct support trunnion and recorded on a 14-channel oscillograph as an axial-force component (thrust), normal-force component, and moment tending to rotate the duct (pitching moment). Also recorded on the oscillograph are the aircraft angular velocities about the roll, pitch, and yaw axes, as well as lateral-, longitudinal-, and directional-control positions. In addition, a camera was mounted on the top of the vertical tail to record the flow pattern indicated by tufts attached to the right wing during the various flight conditions.

The fuselage angle of attack and the sideslip angle of the aircraft, relative to the flight path, were measured by vanes located on the end of a nose boom. The wing angle of attack was derived by adding the incidence of the wing with respect to the fuselage (2.5°) to the fuselage angle of attack α_f.

Static test rig.- Load cells in the tie-down cables were used to measure induced and control rolling moments during simulated hovering conditions for static rig testing. The load cells were connected to a Brown recorder (fig. 4). Tuft patterns were arranged as an aid in observing the flow about the aircraft in the simulated hovering condition. The tufts were located at specific places on the aircraft itself. In addition, a tuft grid was attached to wires running under the aircraft, passing through the plane of the ducts, and extending approximately 4 feet beyond each duct.

RESULTS AND DISCUSSION

Steady-State Descent Conditions

Steady-state descents were made at various duct angles, fuselage angles of attack, and airspeed combinations to investigate the rate-of-descent limitations and handling characteristics of the test aircraft in the transition region. Data were obtained over a portion of the transition speed range where the stall limitations in the steady-state descents appeared to be the biggest problem; consequently, data were recorded for duct angles of 40°, 49°, and 60°. The data for a duct angle of 60° are presented in figures 5 to 8.

One problem that became immediately apparent from tuft studies during descents was stalling at the outer portion of the wing panels adjacent to the ducts. Figures 5 to 8 are photographs taken from the actual motion-picture data which show the tuft patterns produced by the flow over the wing of the tilt-duct aircraft.

Figure 5 shows the aircraft wing at conditions ranging from level flight to a limiting rate of descent with the duct angle at 60°. The procedure during these descent trials was to hold the airspeed constant and to allow the angle of attack to increase accordingly as power was decreased. This case was considered typical for the limiting combinations of duct angle, velocity, and angles of attack. As shown in figure 5, when the rate of descent is increased, with the

duct angle and airspeed held constant, the angle of attack is increased, and the stalled area on the wing is thereby increased. In figure 5(c), where the fuselage angle of attack is 12° (wing angle of attack of 14.5°) and the rate of descent is 600 feet per minute, the tufts indicate that a major portion of the wing has become stalled.

Two tests were made at a duct angle of 60° by using the alternate method of holding the angle of attack constant and allowing the airspeed to increase proportionately with rate of descent. Figure 6 shows the flow patterns for the first test with a constant wing angle of attack of 6.5°. Figure 6(a) shows the flow over the wing with the aircraft in level flight at a velocity of 37 knots. As the rate of descent was increased to 900 feet per minute (fig. 6(b)) with the wing angle of attack held constant, the flow is shown to become increasingly stalled. As a means of gaging the effect of holding a lower angle of attack in the descent, the second descent was started and the same steady-state descent method was used; the velocity was 47 knots and wing angle of attack, -1.5°. The flow patterns for this test are shown in figure 7. At higher rates of descent at the same duct angle the flow is much smoother over the outer portion of the wing when low angles of attack are maintained (figs. 7(b) and 7(c)). This condition is accomplished, however, at the expense of having to tolerate excessive nose-down attitudes.

The stalled effects encountered during the flight conditions described above are believed to arise from increased vortex action at the lifting ducted fans. The lift distribution across the span (including the ducted fans) is altered because of the lift produced by the ducted-fan units. The increased vortex action at the ducted fans induces a positive angle of attack on the portion of the wing adjacent to the ducts. This induced angle of attack, added to the nominal angle of attack already on the wing, is sufficient to cause stall and flow separation. When this flow condition is obtained during descents or level flight (high angle of attack and high duct angle), increased aircraft motions, particularly about the roll axis, and lateral stick "snatching" were experienced. Although a significant problem area in an aircraft of this type, the stall can be delayed by shifting the lifting load from the wing to the ducted fans so that the combination of wing geometric angle of attack and induced angle of attack is below the stall angle of attack of the wing. The load is shifted from the wings by increasing the duct angle and thereby permits the ducted fans to carry a greater portion of the lift. The possible limitations to be encountered in utilizing combinations of duct angle and steep nose-down attitudes to reduce angle of attack (and hence the flow separation effects) during steep descents are as follows: (1) discomfort in tolerating the attitudes required and (2) doubt concerning the feasibility of recovery from these steep nose-down attitudes prior to touchdown. These limitations indicate a need for further study of these problems with aircraft of this type.

Steady-State Climb Conditions

Figure 8 shows the flow over the wing with the aircraft in a rate of climb of 400 feet per minute, duct angle of 60°, airspeed of 37 knots, and a wing angle of attack of 0.5°. In this condition, the flow over the wing appears to

be very smooth. In addition, pilots report that no difficulty has been experienced in any climb configuration.

Aircraft Motions Resulting From Effects of Flow Separation

Typical time histories of aircraft angular motions and control surface motions resulting from adverse stall over the lifting surface during a steady-state rate of descent are shown in figure 9. Figure 9(a) shows the time histories of the angular velocities and control positions about the three axes when the aircraft is in a level-flight condition. The flow patterns in figure 5(a) were obtained for the same flight as the data for figure 9(a). Figure 9(b) shows the time histories of the angular velocities and control positions about the three axes with the aircraft in a limiting rate-of-descent condition and indicates an increase in the frequency and magnitude of erratic aircraft and control surface motions as compared with those shown in figure 9(a). The stalled area of the wing increases from the level-flight condition to the limiting rate-of-descent condition, as can be seen by comparing figures 5(a) and 5(c). The flow patterns in figure 5(c) were taken for the same flight as the data for figure 9(b). Time histories of the angular velocity and control positions for the other steady-state descent conditions indicate the same trend between the level flight and the limiting rate of descent.

Dynamic Stability Characteristics

Longitudinal oscillations.- Angular velocity responses to longitudinal pulse inputs are presented in figure 10 for duct angles of 7°, 20°, 30°, and 50°. In all of these configurations the data indicate stable damping. Pilots' comments indicated that damping of all oscillations was satisfactory. Figure 11 shows the period of the longitudinal oscillation as a function of airspeed in the range of the tests. The data in this curve indicate that the period increases as the duct angle increases (velocity decreases).

Lateral-directional oscillations.- Angular velocity responses to directional pulse inputs are presented in figure 12 for duct angles of 0°, 20°, 30°, 40°, and 50°. The damping in this portion of the transition speed range was stable. Figure 13 presents the period as a function of airspeed for the five duct angles investigated. It may be noted from this figure that the directional oscillatory period also increases as the airspeed decreases. No Dutch roll oscillations were noted by the pilots at these duct angles, and the damping of all oscillations encountered was satisfactory.

Static Stability Characteristics

Apparent dihedral.- Dihedral effect of the tilting ducted-fan aircraft was measured in the level-flight configuration at duct angles of 0°, 20°, 30°, 40°, and 50°. Flight test results, presented in figures 14 and 15, indicate apparent static lateral stability in the ranges of the tests. The apparent static lateral stability was more satisfactory at the lower duct angles and became less

satisfactory as the duct angle was increased. Pilots indicated that the effective dihedral was marginally acceptable for the 0° duct angle condition; however, it became increasingly unsatisfactory as the duct angle was increased. The lower static stability was probably objectionable primarily because of the inadequate roll control power of the configuration. The lateral control surfaces (deflection of the inlet guide vanes) are phased in and out as the duct angle varies (airspeed changes) so that the apparent lateral static stability becomes a function of the changing control power. Consequently, an apparent static stability rather than true static stability is represented in the figures. Figure 15 shows the variation of apparent static lateral stability with airspeed in the level-flight configuration where the average slopes from figure 14 are plotted for each airspeed.

Apparent directional stability.- The apparent static directional stability characteristics of the test aircraft for a speed range of 46 knots to 96 knots were investigated in the level-flight configuration and the results are shown in figures 16 and 17. The duct-angle settings used include the same settings of 0°, 20°, 30°, 40°, and 50° that were used for the other effects. Data shown in figure 16 indicate stable characteristics over the range of the tests. Pilots reported that the directional stability was satisfactory for the high speed end of the transition speed range; however, as the airspeed was decreased the reduced directional stability was unsatisfactory probably because of the inadequate directional control power as the airspeed was decreased. Figure 17 is a plot of the slopes from figure 16 as a function of airspeed and shows the greater apparent static directional stability in the high speed (low-duct-angle) range, which becomes less as the airspeed is decreased through duct angle rotation.

Hovering Characteristics

Hovering flight.- Qualitative investigations of the hovering flight characteristics of the tilt-duct research aircraft were performed by two NASA pilots. Control inputs used in these tests were only for the purpose of establishing steady, controlled hovering. The pilots found the aircraft difficult to control about the roll and yaw axes. Even when the aircraft was high enough to be above ground-interference effects, pilots considered it hazardous to attempt trial roll-control inputs because of the long time delay in achieving rolling velocity and the inability to stop it within safe attitude limits.

The ratios of the control power to inertia were too low about the roll and yaw axes according to the criteria of reference 6 and, in keeping with this fact, a very slow response to corrective yaw and roll control inputs was experienced. (The ratios of control power to the inertia were estimated to be 0.06 radian/sec^2 per inch of stick displacement for the roll axis and 0.2 radian/sec^2 per inch of pedal displacement for the yaw axis. These ratios represent approximately 1/6 of the roll and 1/10 of the yaw control required to meet the minimum acceptable criteria of ref. 6.) In some cases, when the pilots attempted to correct for a yawing velocity or a yaw displacement near the ground, full application of corrective control was not sufficient to prevent turning 90° or more in heading. This characteristic was reported by both pilots. When lateral control was applied to correct a rolling velocity, response was judged to be dangerously sluggish. In some cases, roll displacement, apparently owing, in part, to ground interference,

could not be corrected with full lateral control before contacting the ground. Control power about the pitch axis was judged adequate, at least for research testing. (The ratio of control power to inertia about the pitch axis was estimated to be 0.1 radian/sec^2 per inch of stick displacement or approximately that required to meet the minimum acceptable criteria of ref. 6.) Reference 7 presents pilots' observations on these problems.

Tethered hovering flight.- Attempts to obtain data that would define the rolling-moment characteristics of the tilt-duct aircraft in a simulated hovering condition were not completely successful; however, some useful information was extracted from these tests. Tufts attached to wires running beneath the aircraft through the plane of the ducts, as discussed in the Apparatus and Procedure section of this paper, indicated asymmetrical flows under the wing with bank angle which contributed to unstable tendencies of this aircraft about the roll axis in the hovering condition. Figure 18 is a sketch describing the direction of flow from the ducted fans during a typical condition investigated.

CONCLUSIONS

Flight investigations on the tilt-duct VTOL research aircraft indicate the following conclusions:

1. Useful rates of descent over the range of duct angles investigated (duct angles from 40° to 60°) are limited in the research vehicle because of wing stall, even though the wing is carrying only part of the lift. The increase of flow separation on the wing during high rates of descent causes an increase in the erratic, non-control-induced, aircraft angular velocities. When the lifting surfaces are kept at low angles of attack by shifting the load to the ducts, steep approaches may be possible without encountering adverse stall effects over the wing. The tolerability of the resulting steep nose-down attitudes, however, should be investigated in future flight studies. This flow separation problem could also be lessened by using various stall delay devices.

2. Hovering flight on the test vehicle is considered dangerous because of inadequate control power about the roll and yaw axes and thus illustrates the applicability of existing helicopter control requirements to an aircraft of this type.

3. Simulated hovering in a static test rig indicates unstable rolling moment with roll attitude due to asymmetrical flow in the presence of the ground. Designers should be fully aware of this phenomenon when considering a similar configuration.

4. Longitudinal and lateral-directional oscillations, resulting from pulse inputs over a duct angle range of 0° to 50°, are damped. Pilots' comments indicated that the degree of damping is satisfactory. In both the longitudinal and lateral-directional cases the period increases as the airspeed decreased.

5. According to pilots' comments, the aircraft appears to have lateral and directional stability over the transition speed range, but becomes less stable to an undesirable degree at the higher duct angles (lower airspeeds). Inadequate

control power about the roll and yaw axes probably influences the pilots' comments considerably.

Langley Research Center,
National Aeronautics and Space Administration,
Langley Station, Hampton, Va., July 26, 1962.

REFERENCES

1. Tapscott, Robert J., and Kelley, Henry L.: A Flight Study of the Conversion Maneuver of a Tilt-Duct VTOL Aircraft. NASA TN D-372, 1960.

2. Thomas, Lovic P., III: A Flight Study of the Conversion Maneuver of a Tilt-Wing VTOL Aircraft. NASA TN D-153, 1959.

3. Pegg, Robert J.: Summary of Flight-Test Results of the VZ-2 Tilt-Wing Aircraft. NASA TN D-989, 1962.

4. Yaggy, Paul F., and Mort, Kenneth W.: A Wind-Tunnel Investigation of a 4-Foot-Diameter Ducted Fan Mounted on the Tip of a Semispan Wing. NASA TN D-776, 1961.

5. Yaggy, Paul F., and Goodson, Kenneth W.: Aerodynamics of a Tilting Ducted Fan Configuration. NASA TN D-785, 1961.

6. Tapscott, Robert J.: Helicopters and VTOL Aircraft - Criteria for Control and Response Characteristics in Hovering and Low-Speed Flight. Aero/Space Eng., vol. 19, no. 6, June 1960, pp. 38-41.

7. Reeder, John P.: Handling Qualities Experience With Several VTOL Research Aircraft. NASA TN D-735, 1961.

TABLE I.- PHYSICAL CHARACTERISTICS OF THE AIRCRAFT

Ducted propellers:	
Diameter, ft	4
Number of blades (each fan)	8
Rotational speed (max), rpm	4,800
Ducts:	
Inside diameter, ft	4
Chord, ft	2.75
Rotation, deg	92
Centerbody:	
Length, ft	5.78
Diameter (maximum), ft	1.33
Pitch trim flaps:	
Span, ft.	4.5
Chord, ft	1.29
Travel, deg	23
Straightening vanes (stators):	
Number of blades (each duct)	9
Length, ft	1.33
Chord, ft	0.5
Wing:	
Span (excluding ducts), ft	16
Overall span (including ducts), ft	25.6
Mean aerodynamic chord, ft	6.08
Airfoil section	Modified NACA 2418
Taper ratio	0.747
Sweep, deg	0
Dihedral, deg	0
Area, sq ft	96
Area of each aileron, sq ft	3.0
Incidence, deg	2.5
Vertical tail:	
Height, ft	5.18
Average chord, ft	2.75
Airfoil section	Modified NACA 0012
Area, sq ft	13.9
Horizontal tail:	
Area, sq ft	28.5
Airfoil section	Modified NACA 0012
Span (projected)	12.0
Dihedral, deg	10
Fuselage length, ft	29.3
Overall length (including boom), ft	31.2
Engine	Lycoming YT-53-L-1 and T-53-L-1A
Weight as flown, lb	3,200
Moments of inertia (approximate):	
Pitch, slug-ft^2	1,500
Roll, slug-ft^2	2,900
Yaw, slug-ft^2	3,100
Center of gravity:	
Forward, percent M.A.C.	25
Rearward, percent M.A.C.	32

TABLE II.- DIMENSIONS AND CHARACTERISTICS OF CONTROL SURFACES

Control	Moment source	Number	Maximum deflection	Chord, in.	Span, in.	Area, sq ft	Miscellaneous
Roll	Ailerons	2	14.7° up 13.5° down	12	37	3.0	Lateral stick travel = ±6 in. (at center of grip)
	Inlet guide vanes	14 each duct	17° total travel	3	18	0.375 each	
Pitch	Elevator	1	26.5° up 24.5° down	M.A.C. = 9	62.7	3.92	Longitudinal stick travel = ±6 in. (at center of grip)
	Pitch-control vane	1	1st segment, 6.7° 2nd segment, 37.5° 3rd segment, 67.7°	1.8 5.2 3.0 } 10	19.5	1.36	Articulated
	Pitch trim flap	2	23°	15.5	54		
Yaw	Rudder	1	26° left 26° right	M.A.C. = 8	57	3.17	Pedal travel = ±3.5 in.
	Yaw-control vane	1	1st segment, 3° 2nd segment, 18° 3rd segment, 37°	1.87 5.2 3.05 } 10	19.5	1.36	Articulated

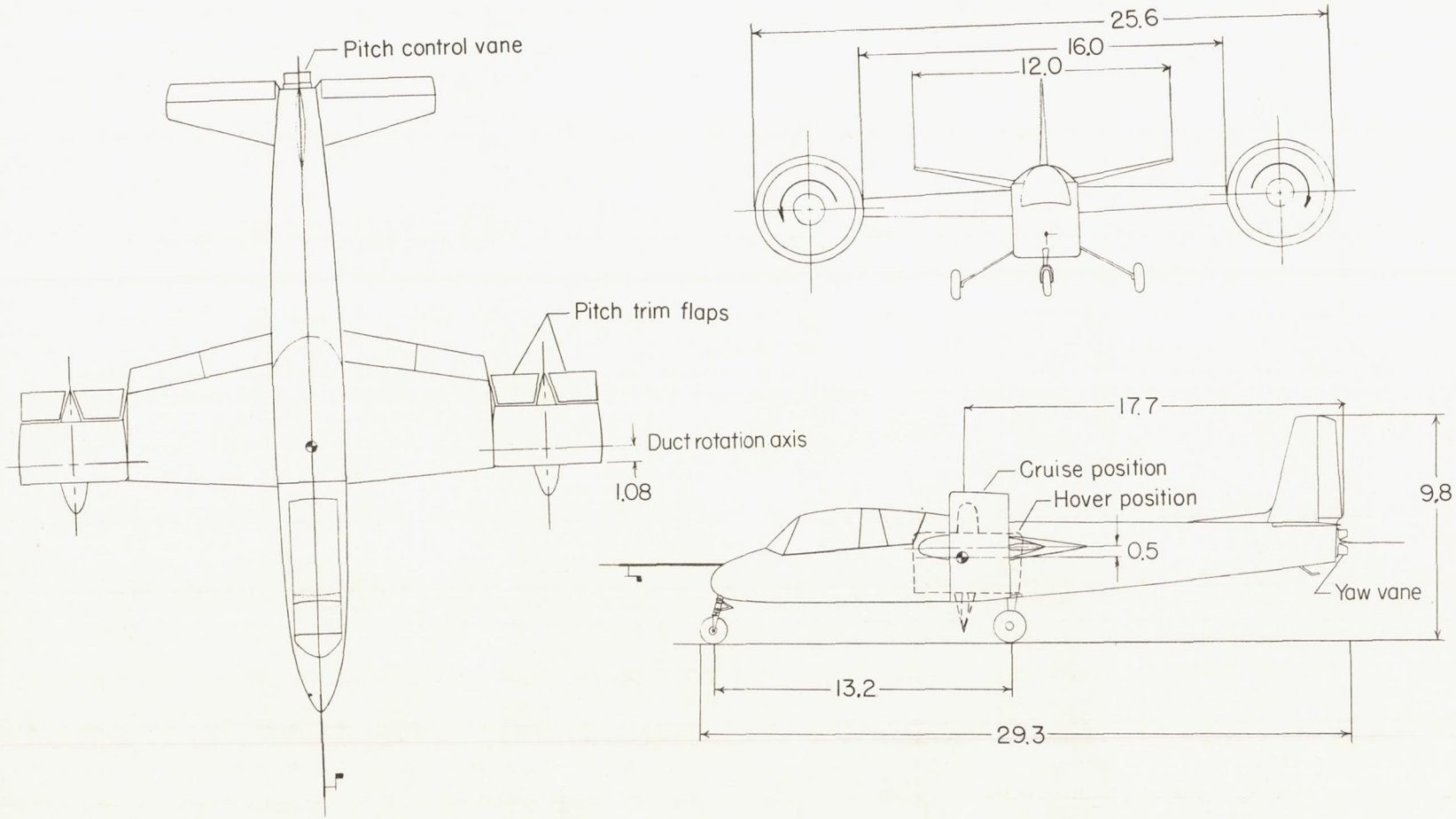

Figure 1.- Sketch of tilt-duct VTOL aircraft. (All dimensions in feet.)

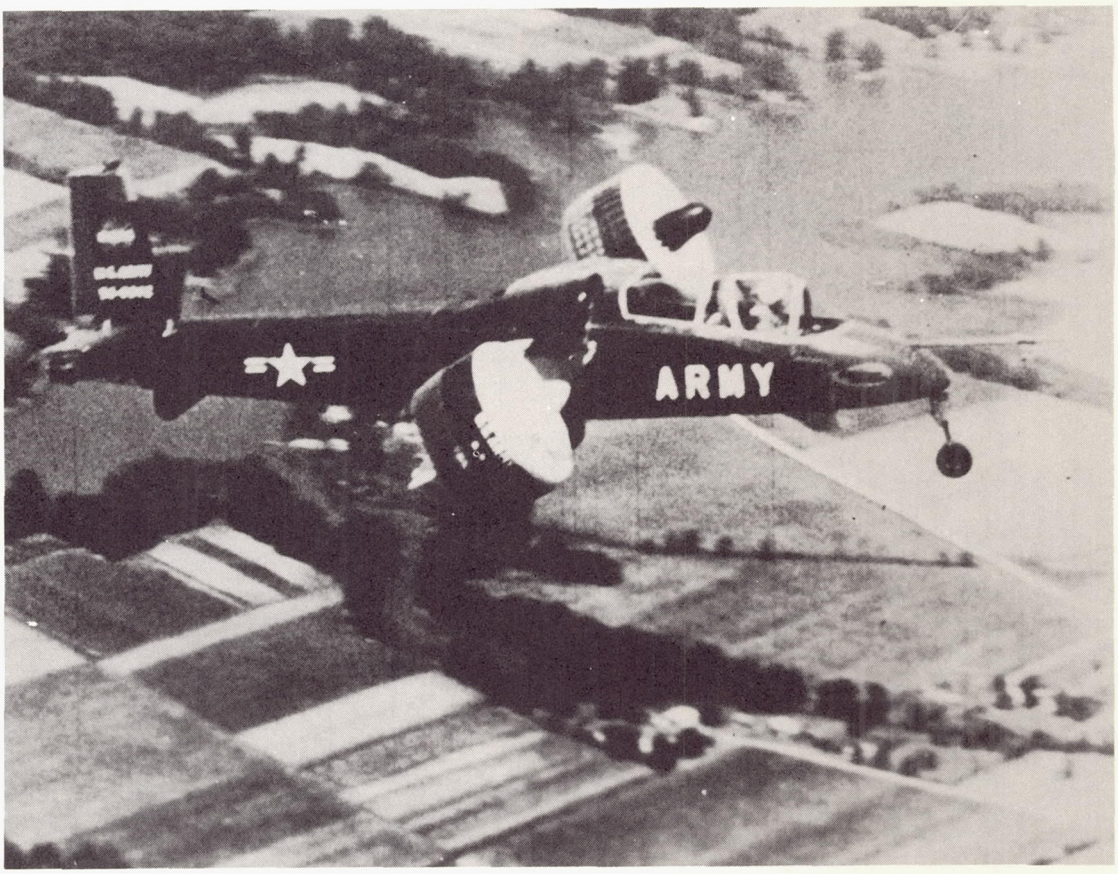

L-62-2124

Figure 2.- Aerial view of the tilt-duct VTOL research aircraft.

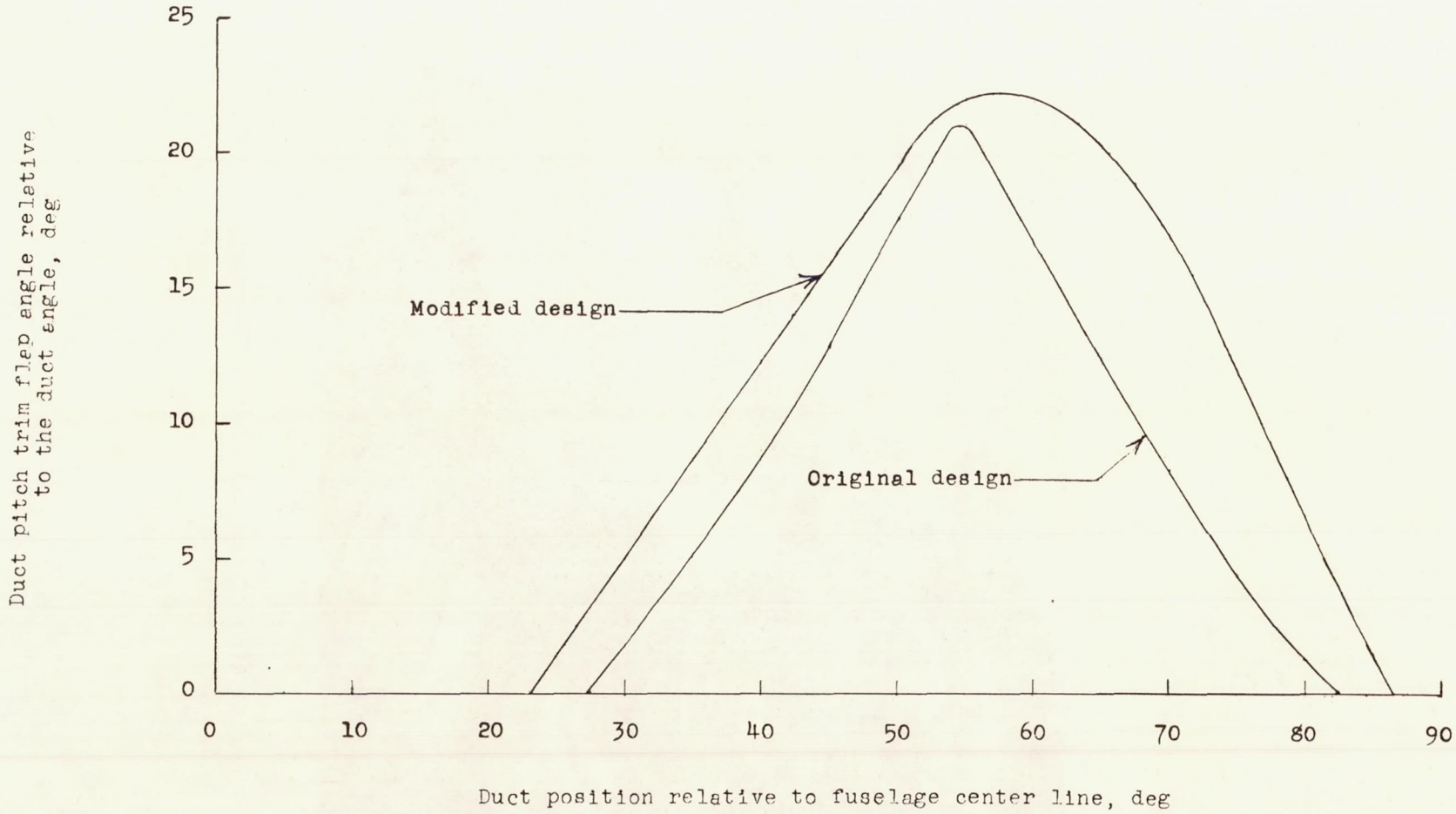

Figure 3.- Programed deflection of the pitch trim flaps with the duct angle using the modified cam design compared with the original cam design.

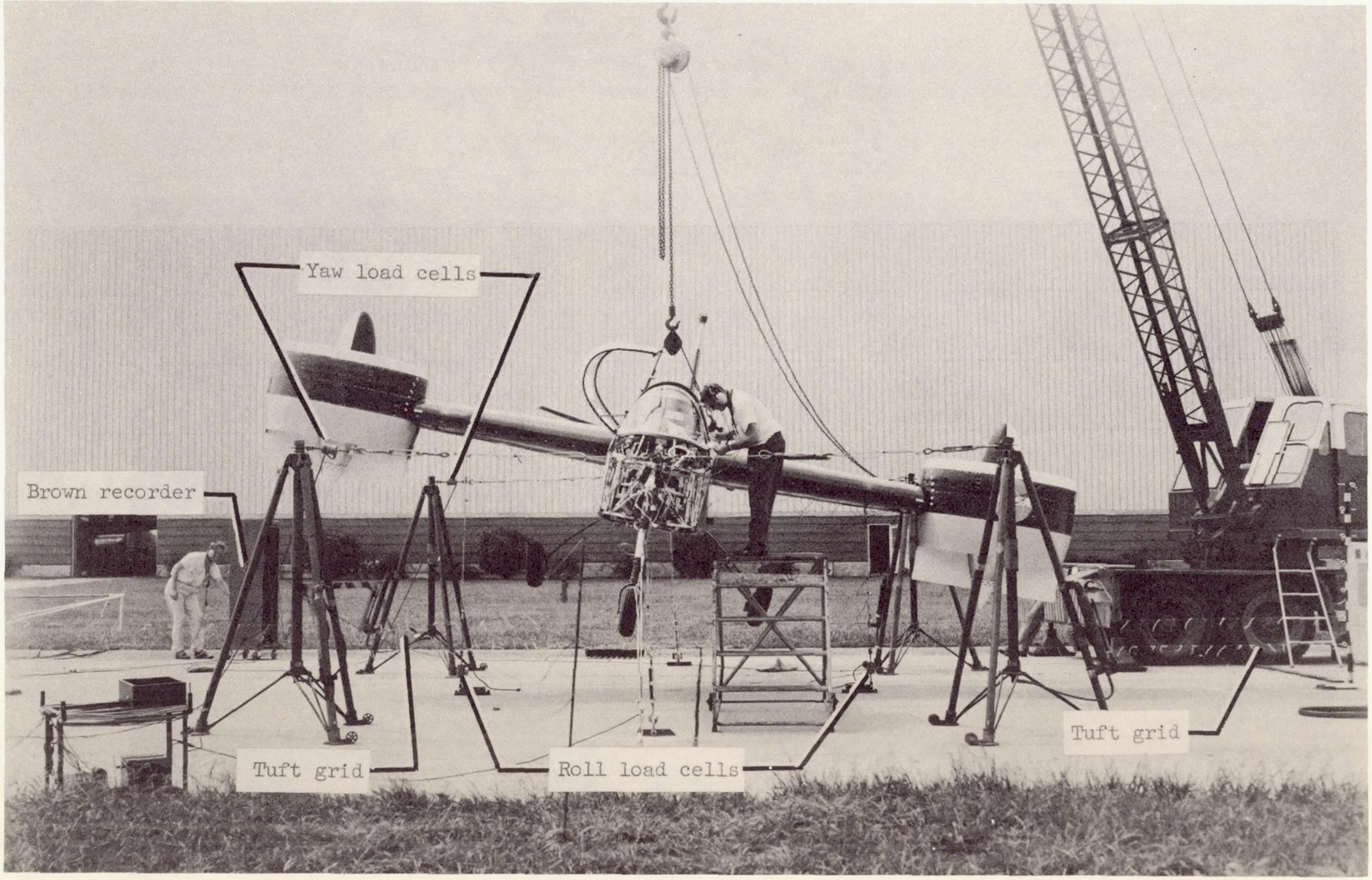

L-60-5902.1

Figure 4.- Hovering static test rig setup for one condition investigated.

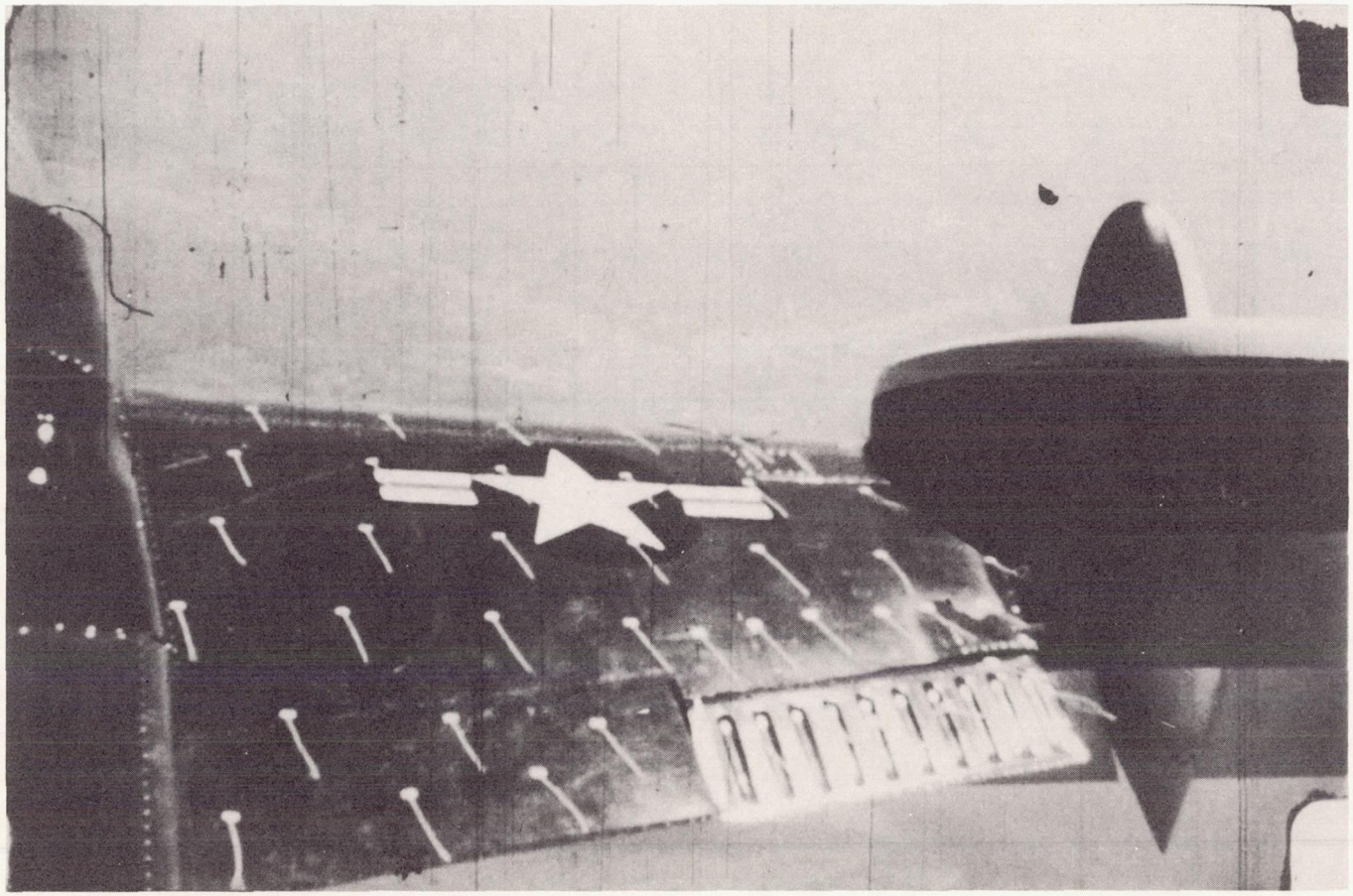

(a) Rate of descent = 0 feet per minute; $\delta_d = 60^\circ$; V = 37 knots; $\alpha_w = 6.5^\circ$. L-62-2113

Figure 5.- Flow over wing during steady-state descent at a constant duct angle and airspeed and varying the fuselage angle of attack and power.

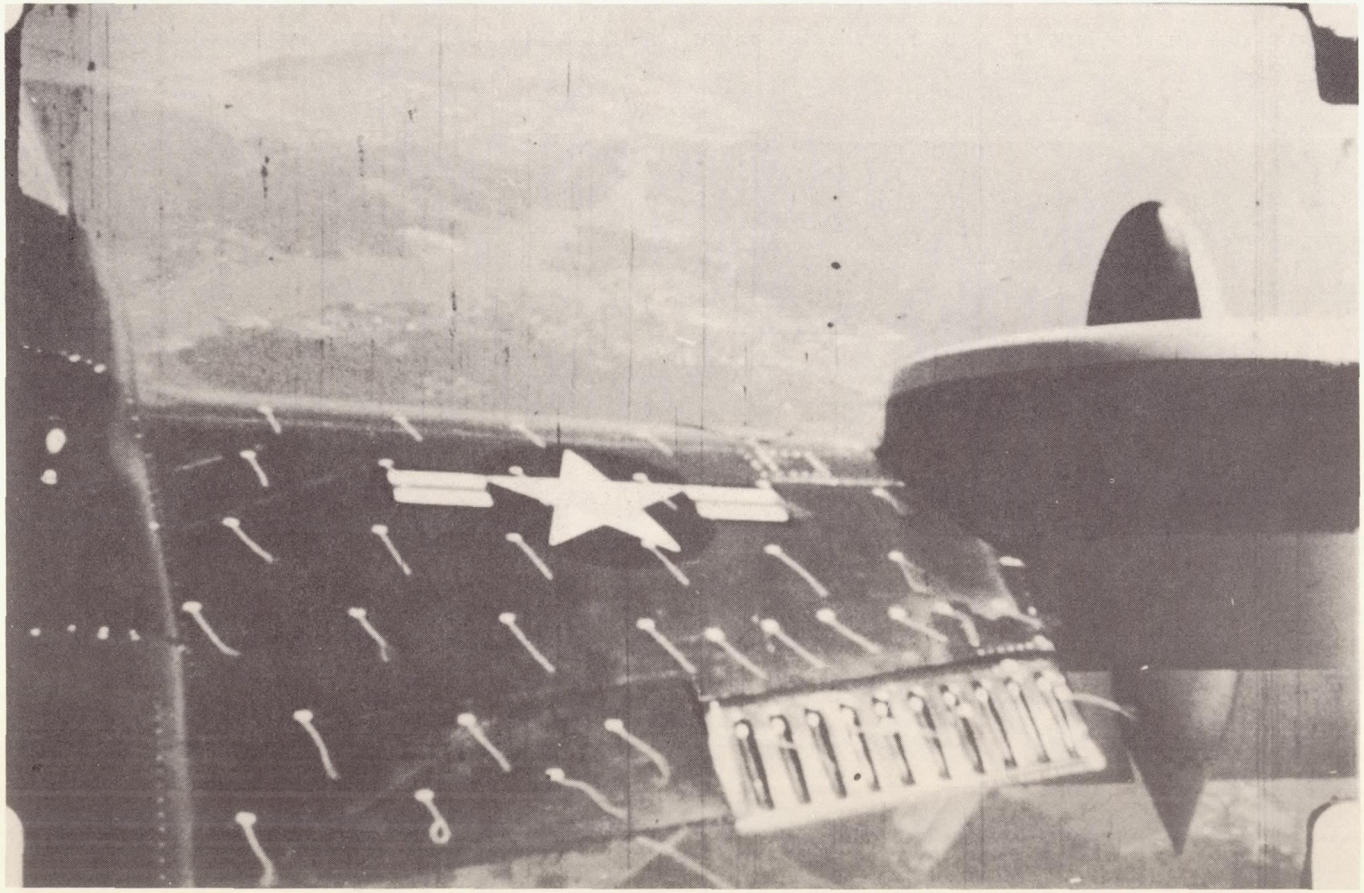

L-62-2114

(b) Rate of descent = 300 feet per minute; $\delta_d = 60^\circ$; V = 37 knots; $\alpha_w = 11.5^\circ$.

Figure 5.- Continued.

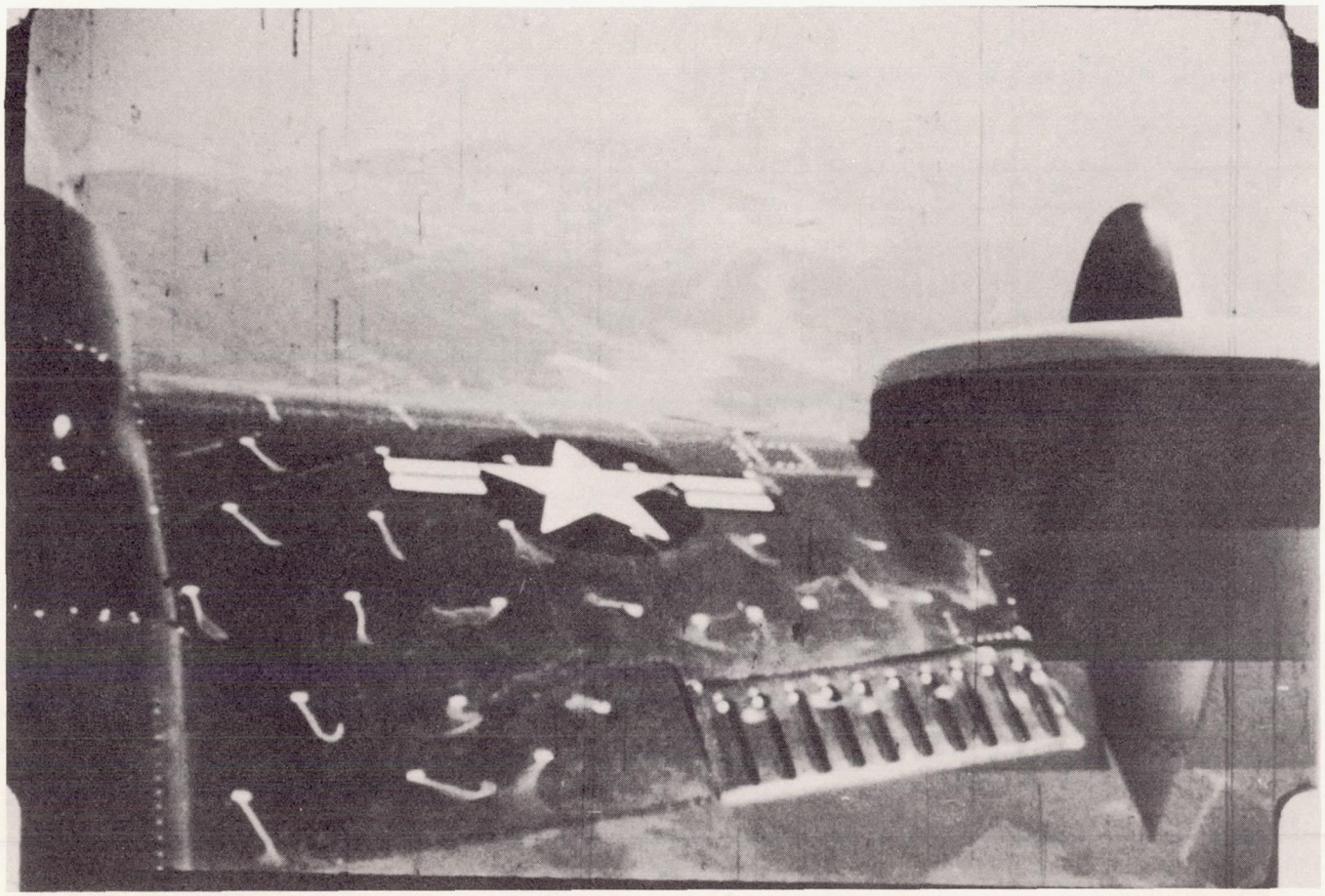

L-62-2115

(c) Limiting rate of descent = 600 feet per minute; $\delta_d = 60^\circ$; V = 37 knots; $\alpha_w = 14.5^\circ$.

Figure 5.- Concluded.

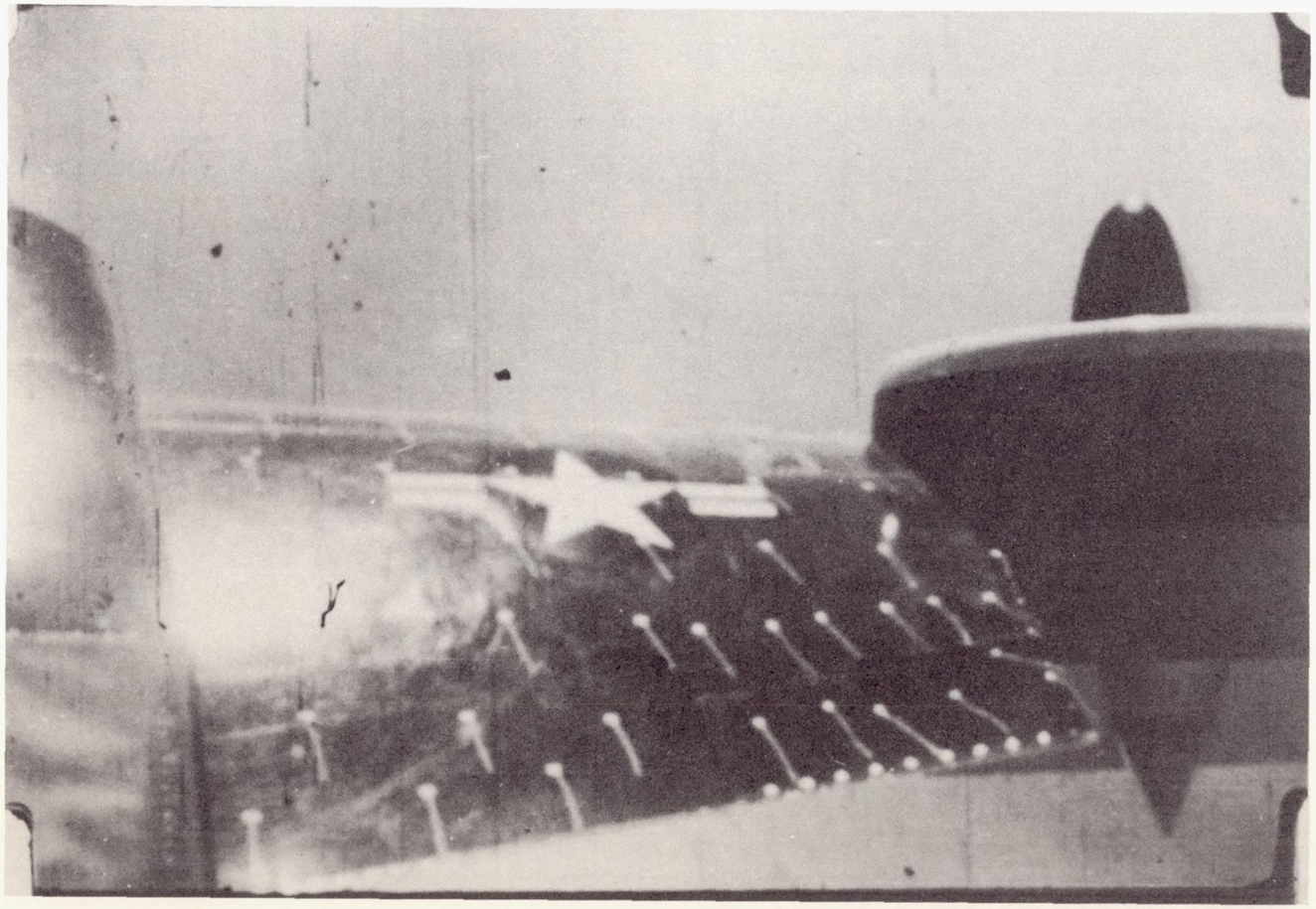

(a) Rate of descent = 0 feet per minute; $\delta_d = 60^\circ$; V = 37 knots; $\alpha_w = 6.5^\circ$. L-62-2116

Figure 6.- Flow over wing during steady-state descent at a constant fuselage angle of attack and duct angle, and varying the airspeed and power.

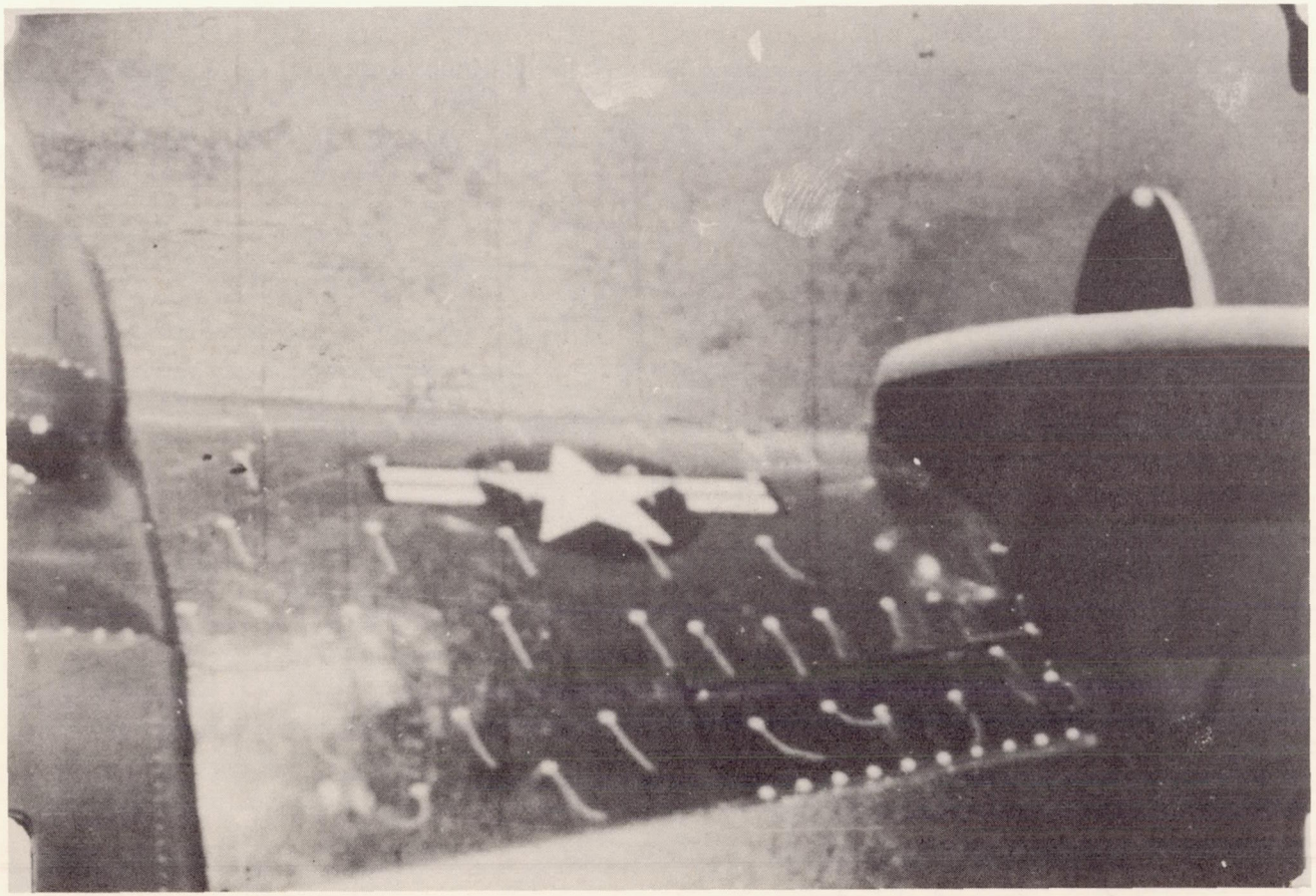

L-62-2117

(b) Limiting rate of descent = 900 feet per minute; $\delta_d = 60^\circ$; V = 46 knots; $\alpha_w = 6.5^\circ$.

Figure 6.- Concluded.

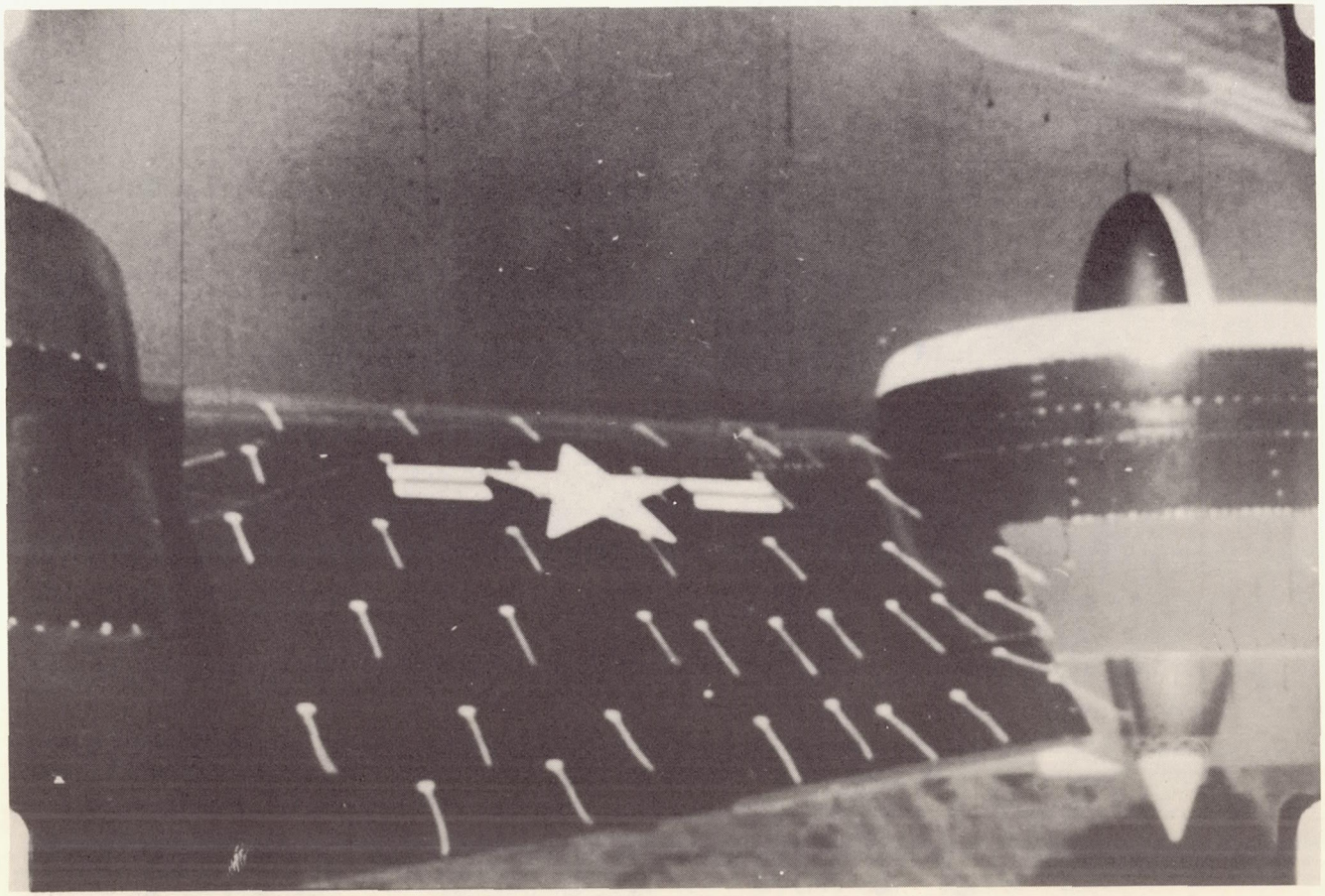

L-62-2118

(a) Rate of descent = 0 feet per minute; $\delta_d = 60^\circ$; V = 47 knots; $\alpha_w = -1.5^\circ$.

Figure 7.- Flow over wing during steady-state descent at a constant duct angle and fuselage angle of attack, and varying the airspeed and power.

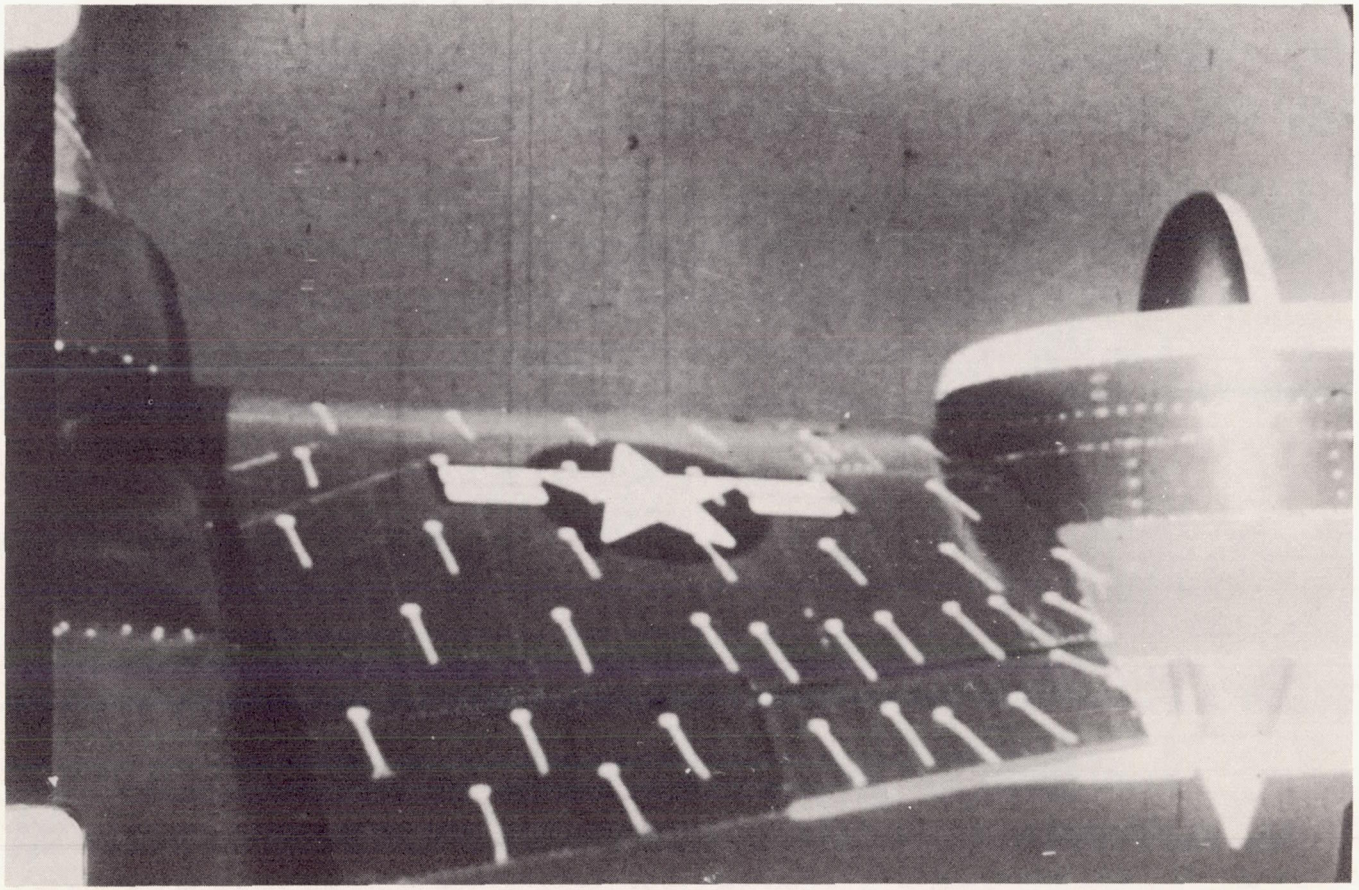

L-62-2119

(b) Rate of descent = 900 feet per minute; $\delta_d = 60^\circ$; V = 55 knots; $\alpha_w = -1.5^\circ$.

Figure 7.- Continued.

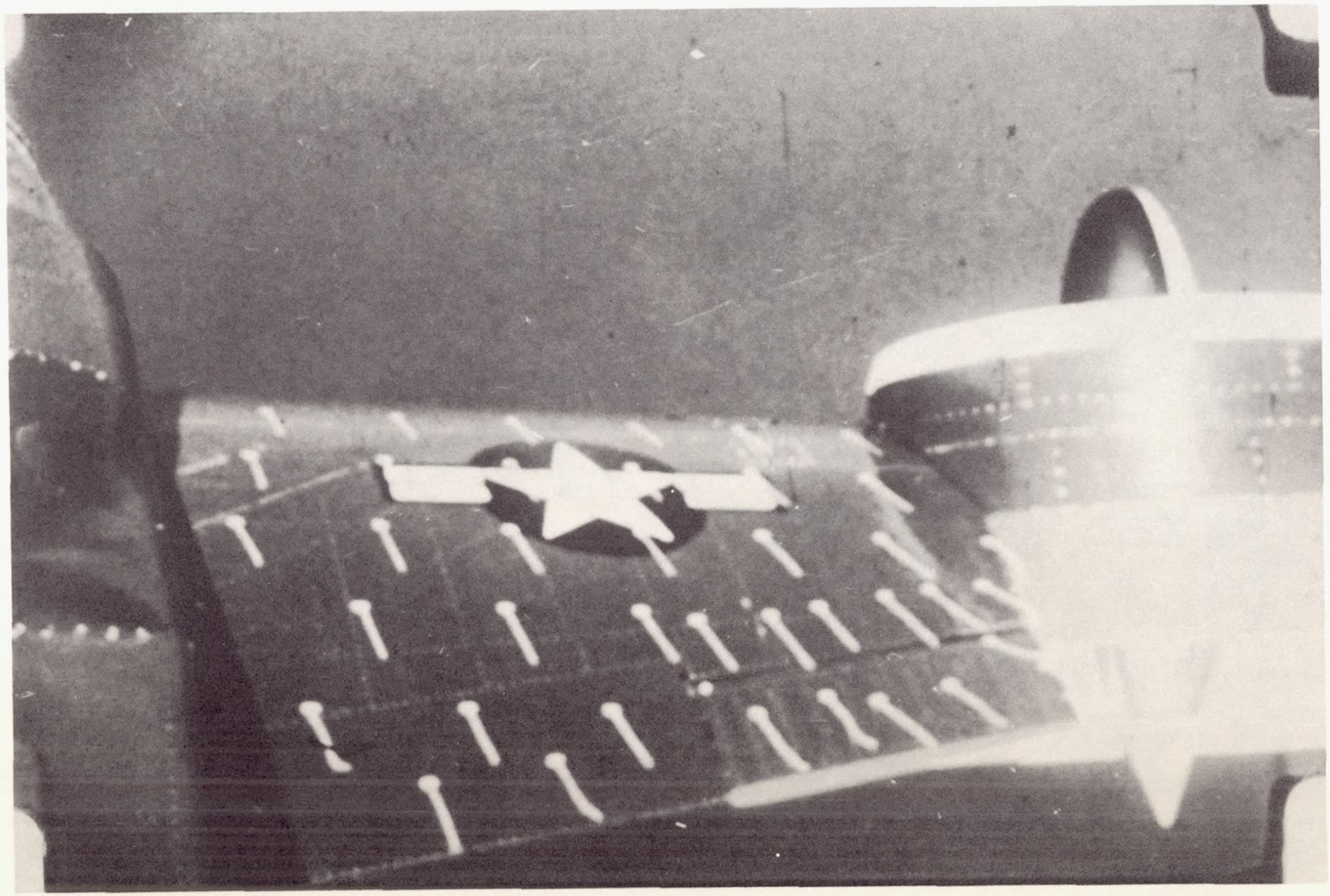

L-62-2120

(c) Rate of descent = 1,200 feet per minute; $\delta_d = 60^\circ$; V = 57 knots; $\alpha_w = -1.5^\circ$.

Figure 7.- Concluded.

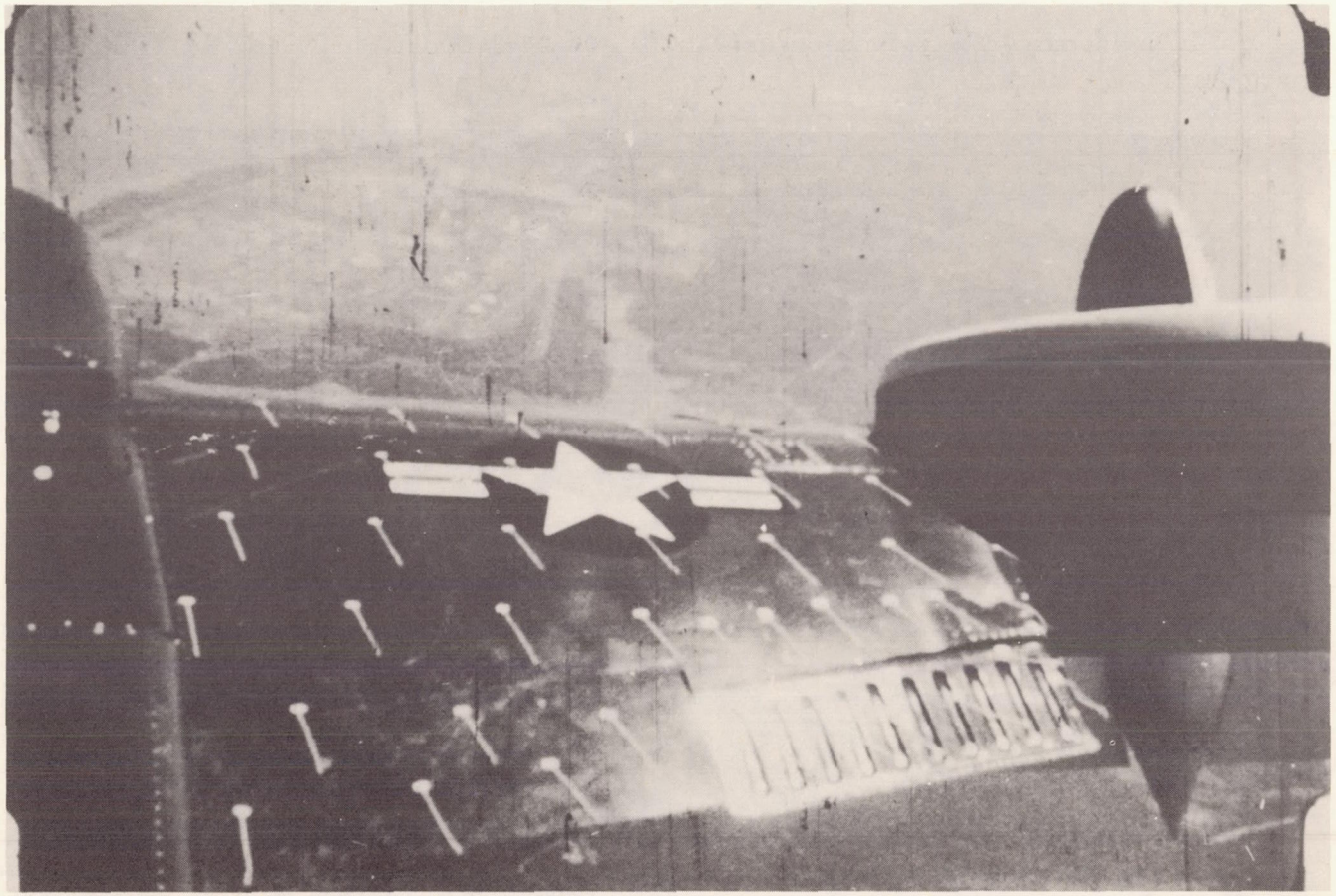

L-62-2121

Figure 8.- Flow over wing during climb maneuver. Rate of climb = 400 feet per minute; $\delta_d = 60^\circ$; V = 37 knots; $\alpha_w = 0.5^\circ$.

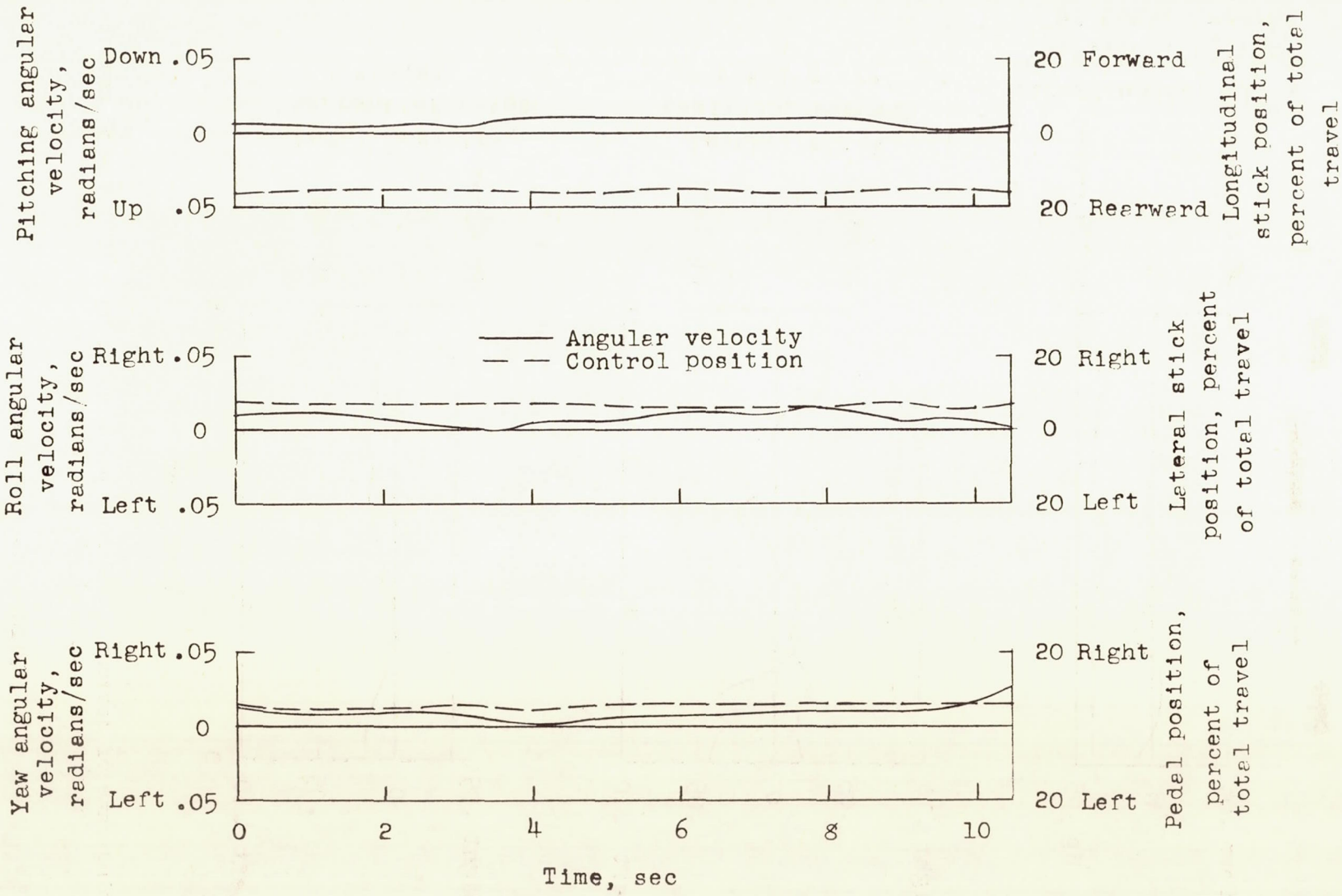

(a) Rate of descent = 0 feet per minute; $\delta_d = 60^\circ$; V = 37 knots; $\alpha_w = 6.5^\circ$; P = 665 hp.

Figure 9.- Time histories of angular velocities and control positions during level flight and limiting steady-state descent.

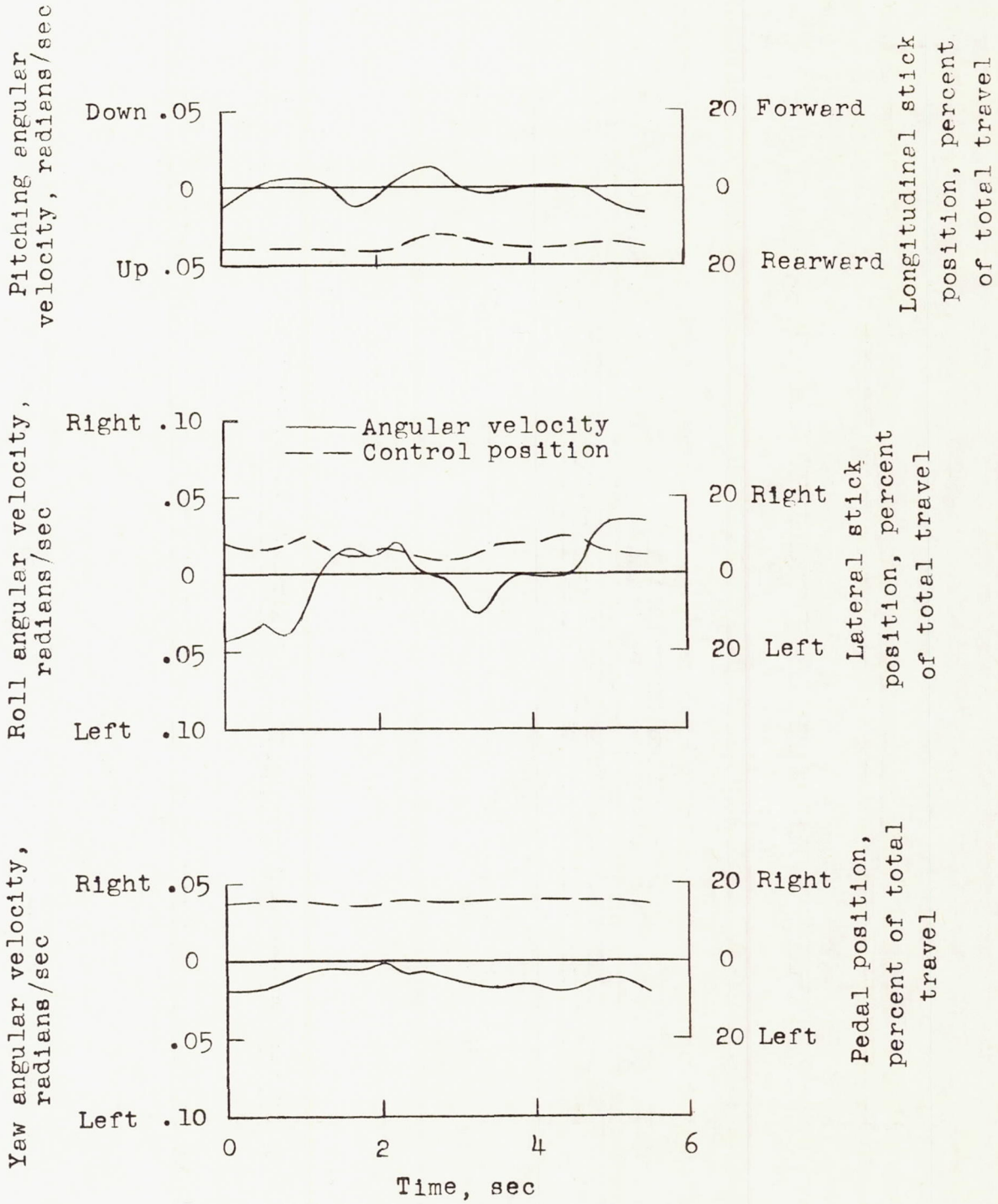

(b) Limiting rate of descent = 600 feet per minute; $\delta_d = 60^\circ$; V = 37 knots; $\alpha_w = 14.5^\circ$; P = 479 hp.

Figure 9.- Concluded.

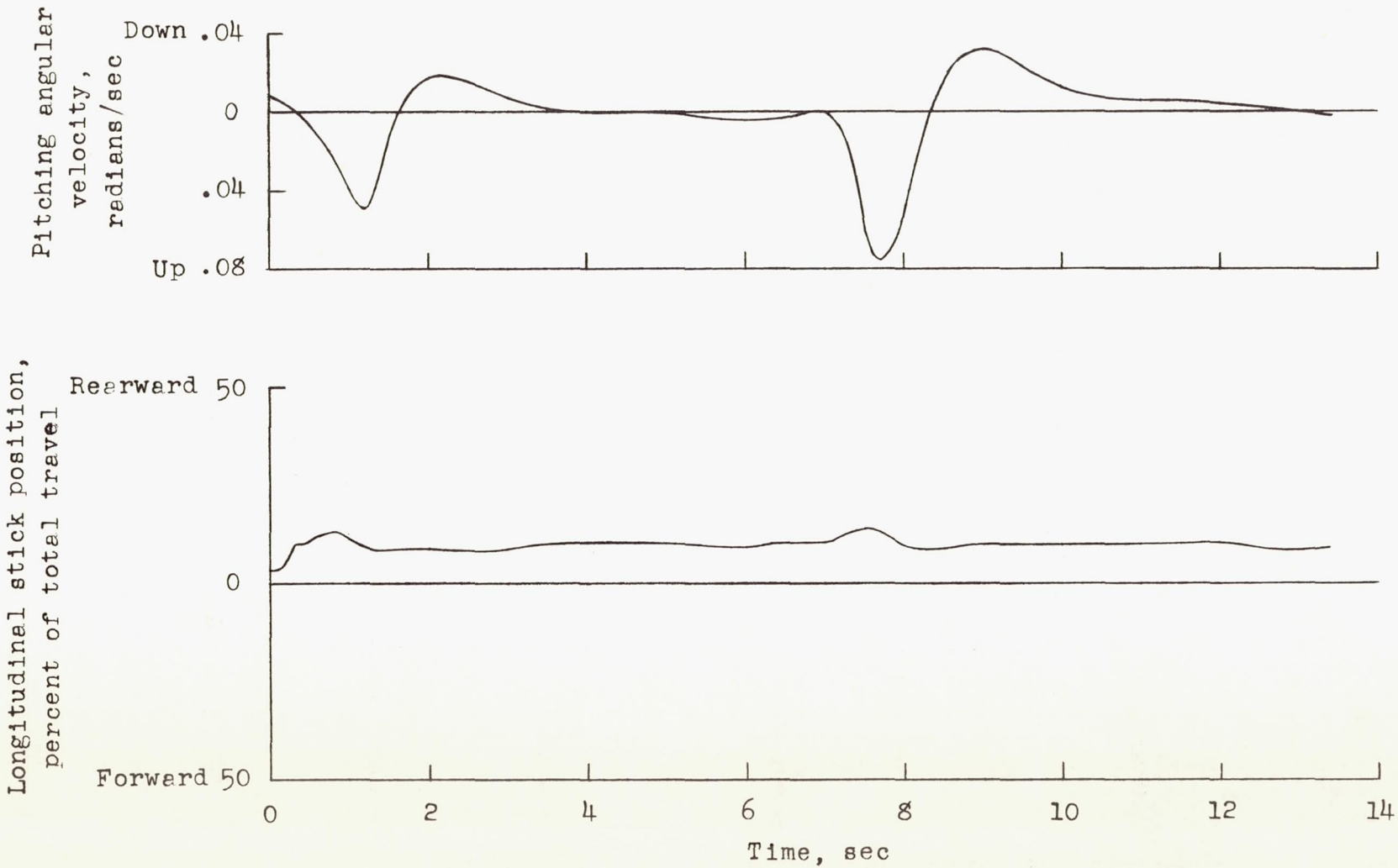

(a) $\delta_d = 7^\circ$; V = 114 knots; P = 303 hp.

Figure 10.- Typical oscillations resulting from longitudinal pulse inputs for several duct angles.

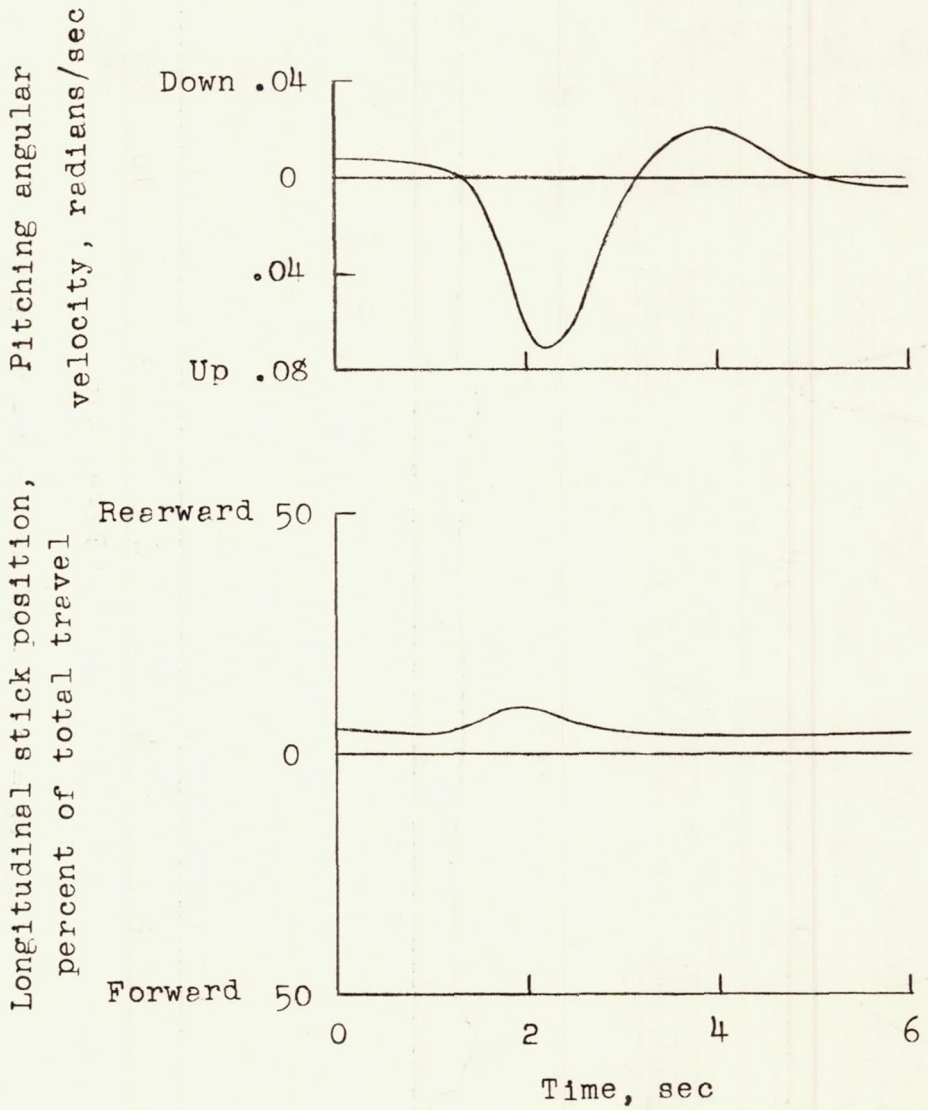

(b) $\delta_d = 20^\circ$; V = 72 knots; P = 226 hp.

Figure 10.- Continued.

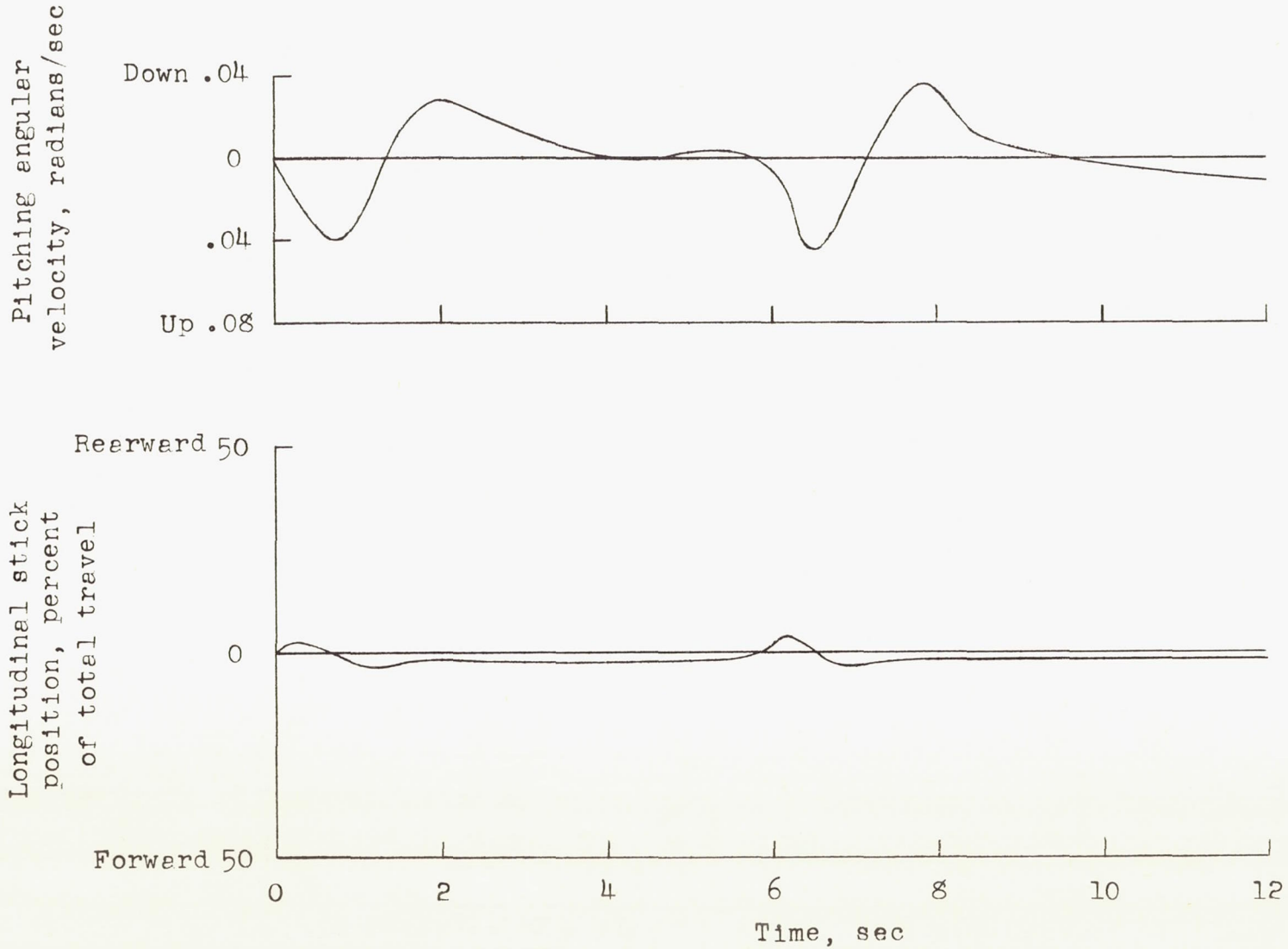

(c) $\delta_d = 30^\circ$; V = 68 knots.

Figure 10.- Continued.

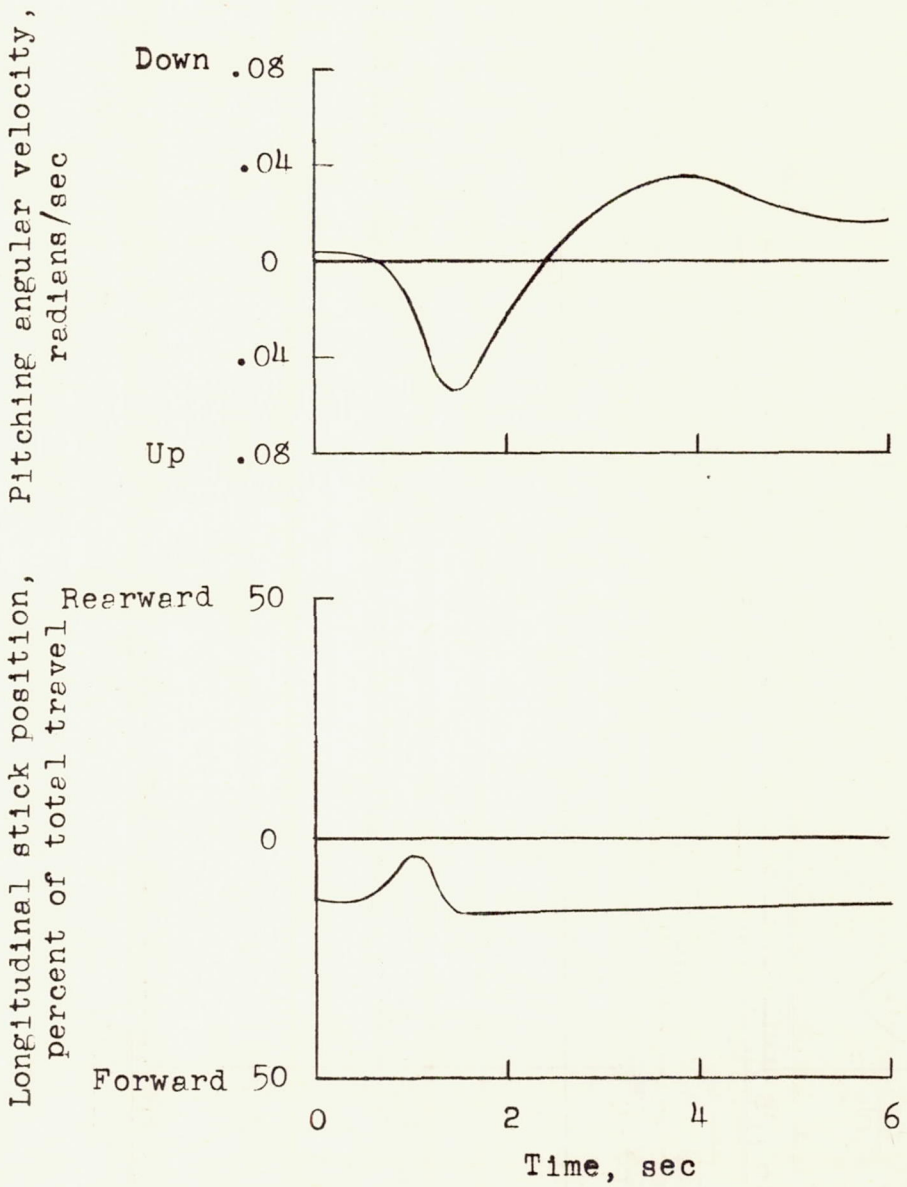

(d) $\delta_d = 50^\circ$; V = 45 knots; P = 578 hp.

Figure 10.- Concluded.

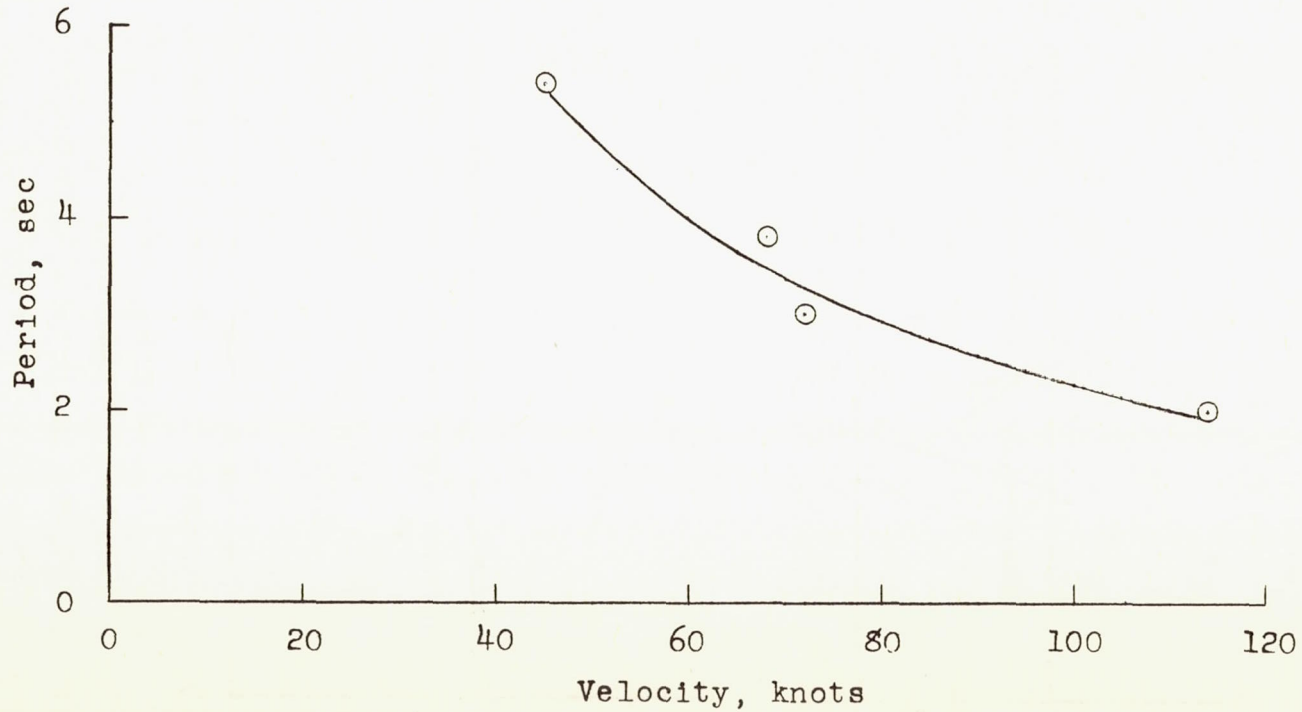

Figure 11.- Variation of the period of longitudinal oscillation with airspeed, level flight.

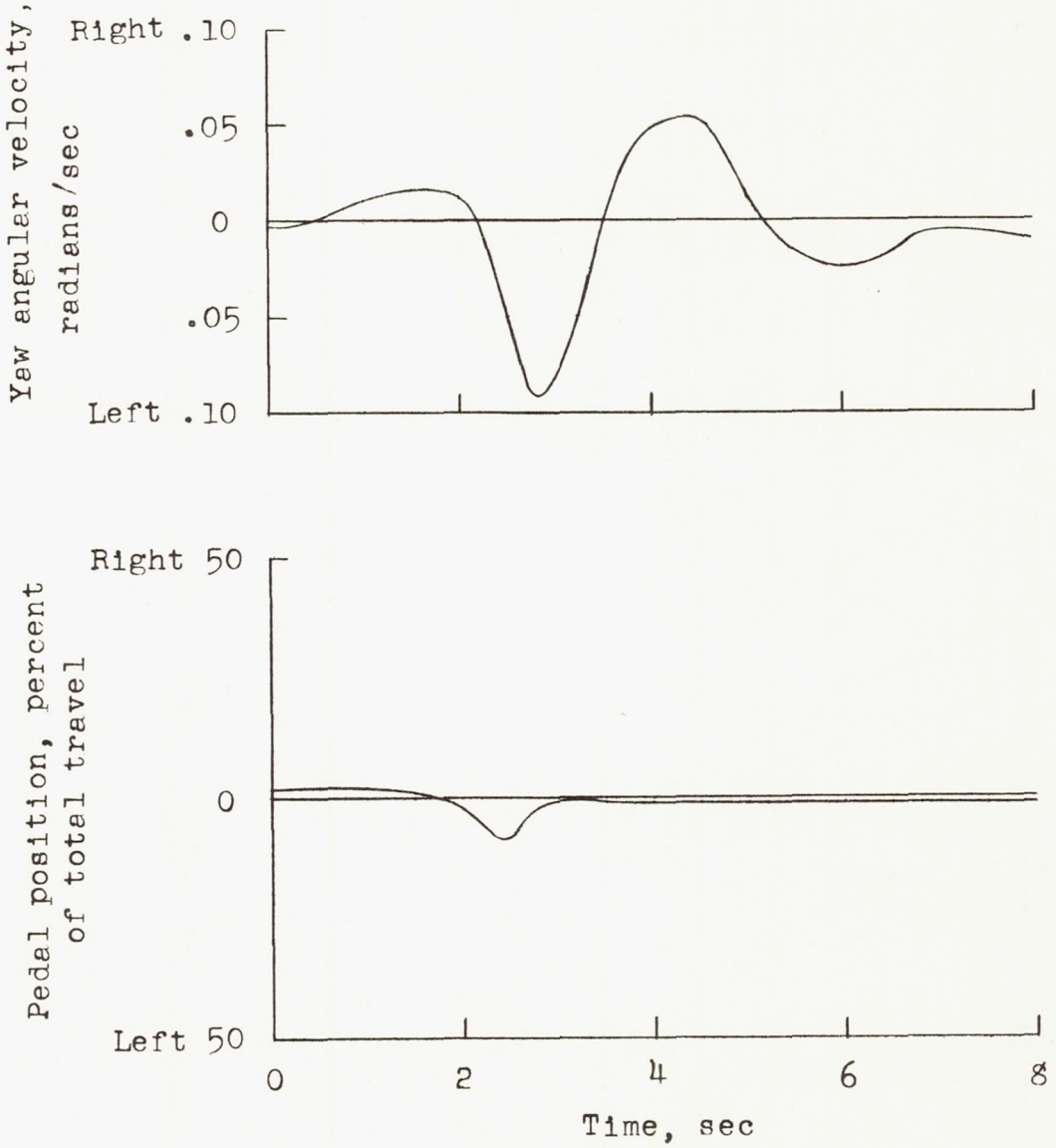

(a) $\delta_d = 0^\circ$; V = 114 knots; P = 302 hp.

Figure 12.- Typical lateral-directional oscillation resulting from directional pulse inputs for several duct angles.

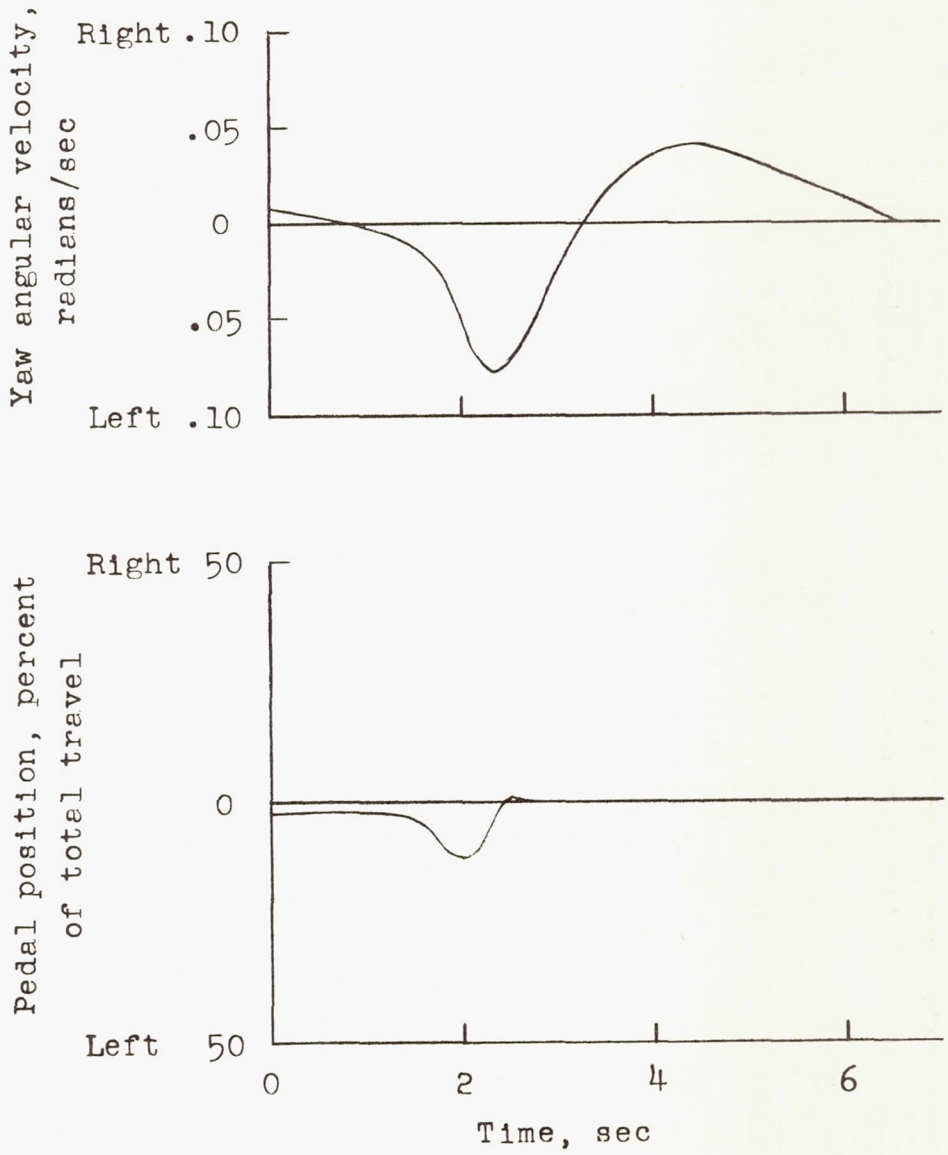

(b) $\delta_d = 20^\circ$; V = 83 knots; P = 254 hp.

Figure 12.- Continued.

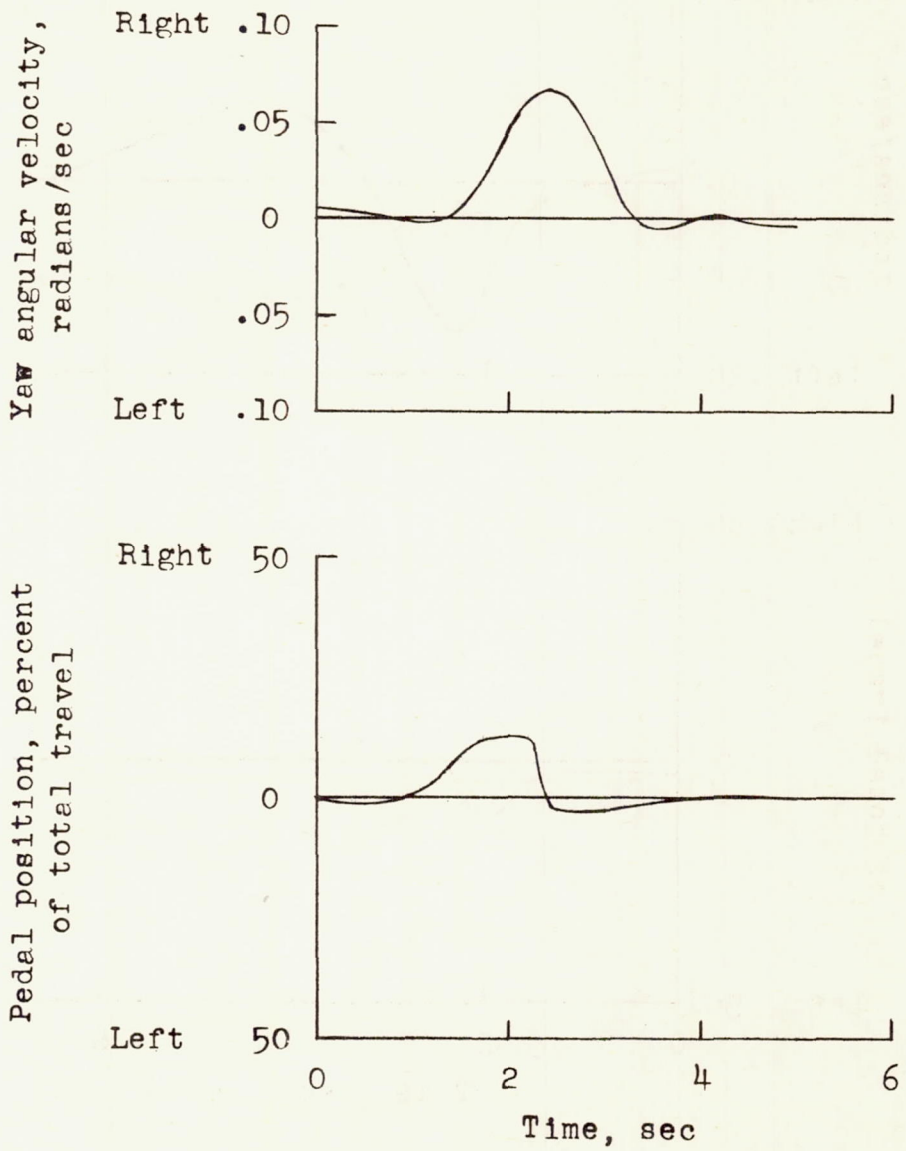

(c) $\delta_d = 30^\circ$; V = 67 knots.

Figure 12.- Continued.

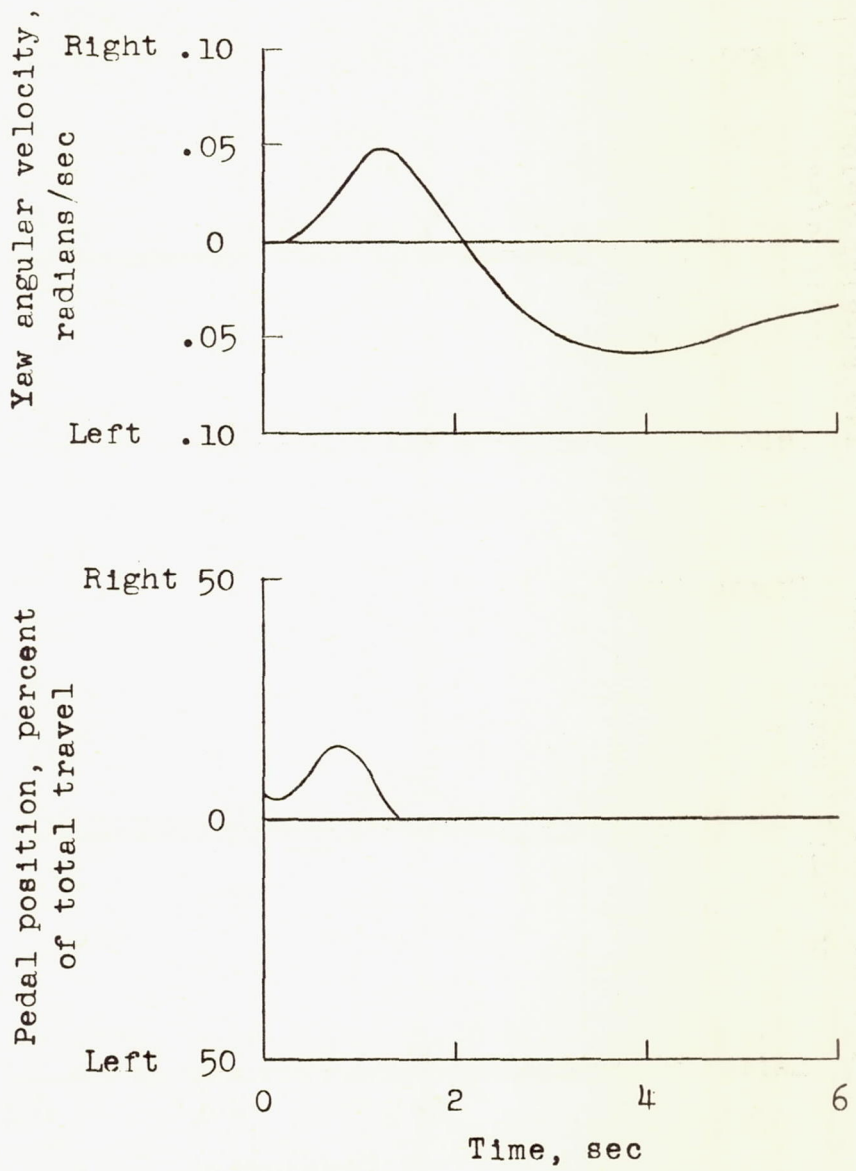

(d) $\delta_d = 40^\circ$; V = 58 knots; P = 423 hp.

Figure 12.- Continued.

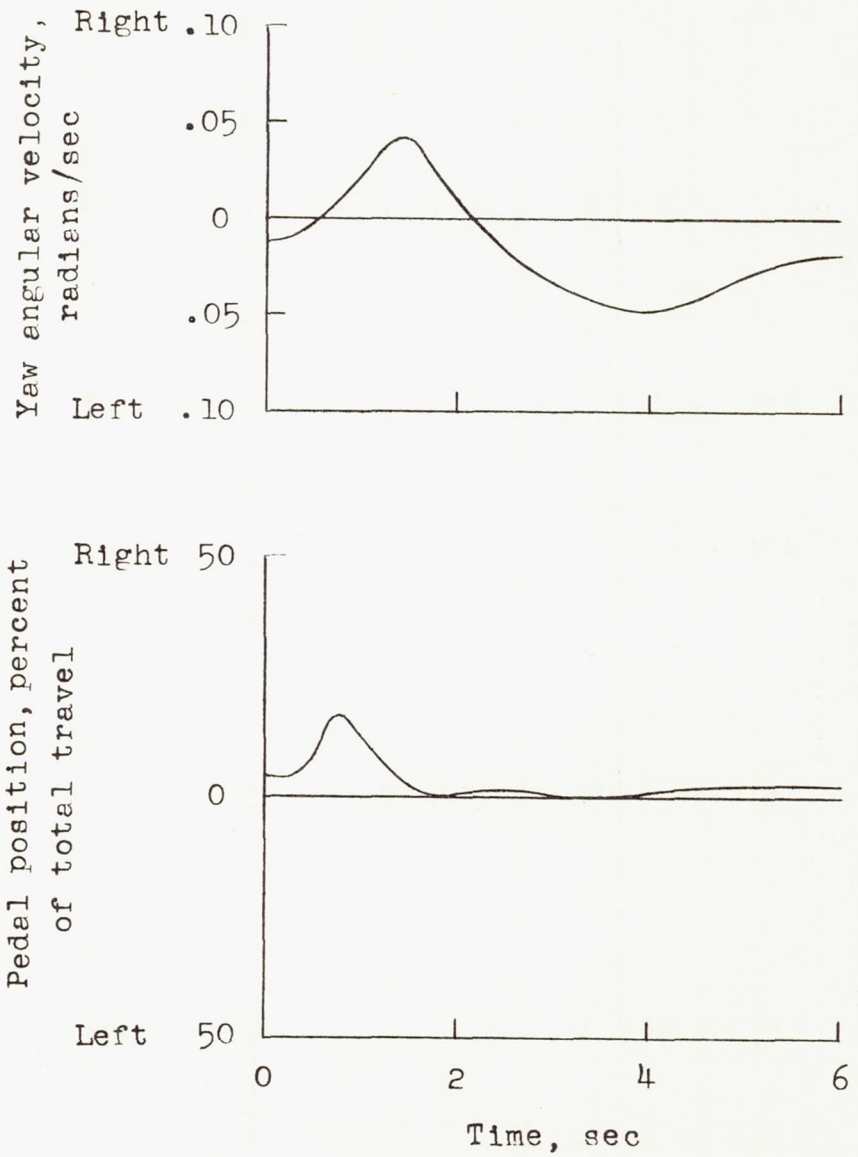

(e) $\delta_d = 50^\circ$; V = 45 knots; P = 578 hp.

Figure 12.- Concluded.

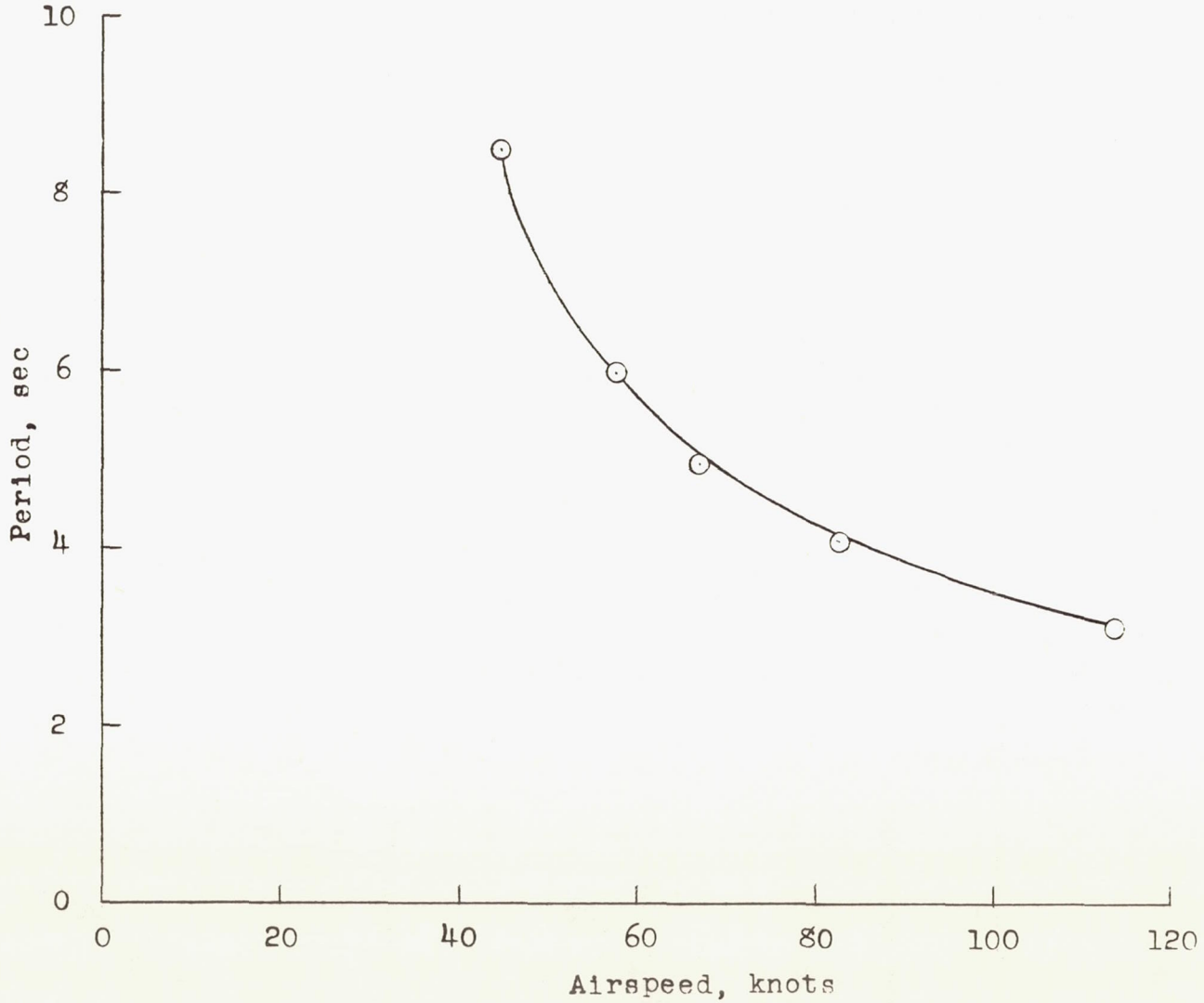

Figure 13.- Variation of the period of lateral-directional oscillation with airspeed, level flight.

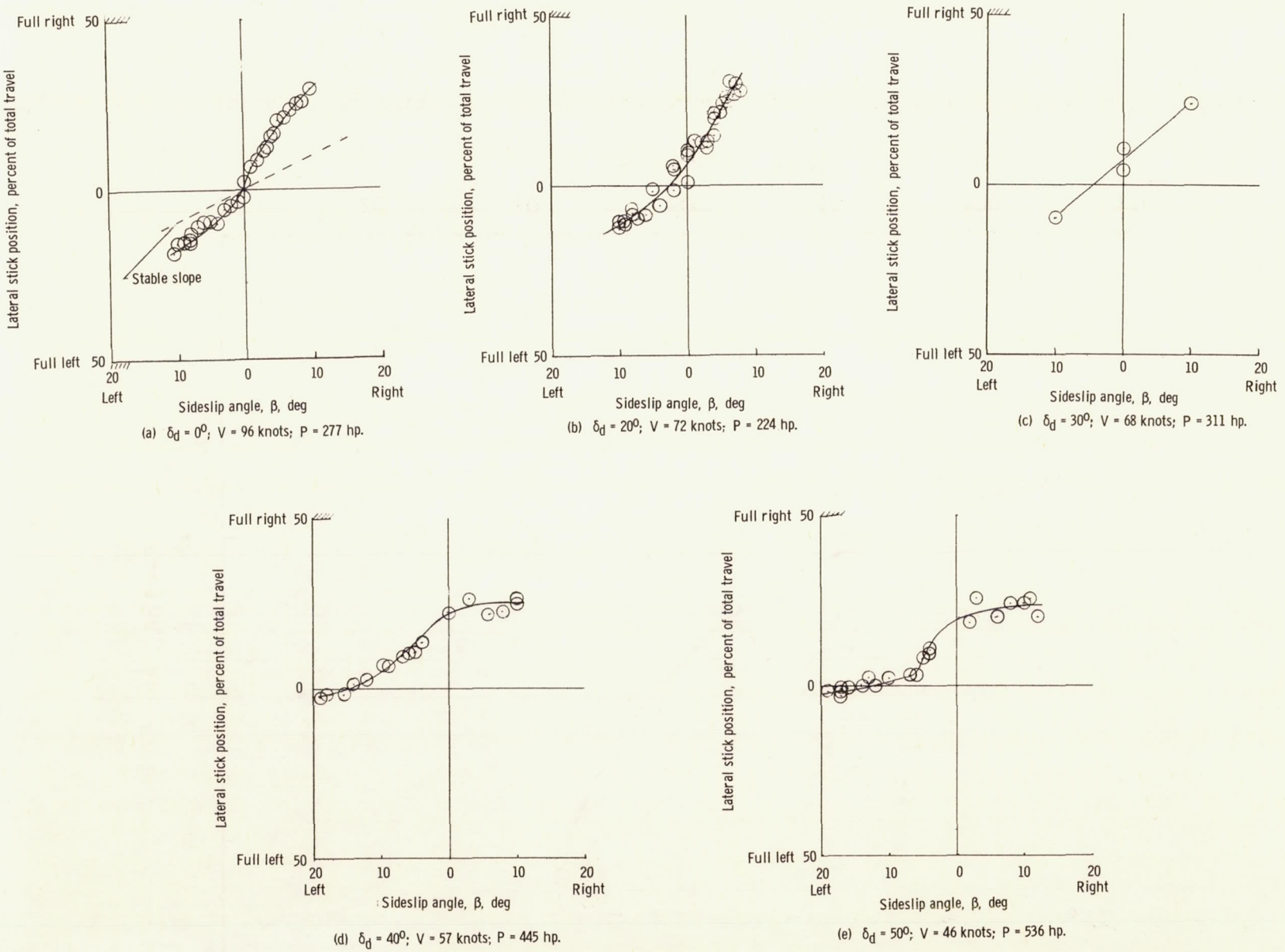

(a) $\delta_d = 0^0$; V = 96 knots; P = 277 hp.

(b) $\delta_d = 20^0$; V = 72 knots; P = 224 hp.

(c) $\delta_d = 30^0$; V = 68 knots; P = 311 hp.

(d) $\delta_d = 40^0$; V = 57 knots; P = 445 hp.

(e) $\delta_d = 50^0$; V = 46 knots; P = 536 hp.

Figure 14.- Apparent dihedral effect from the level-flight configuration at several duct angles.

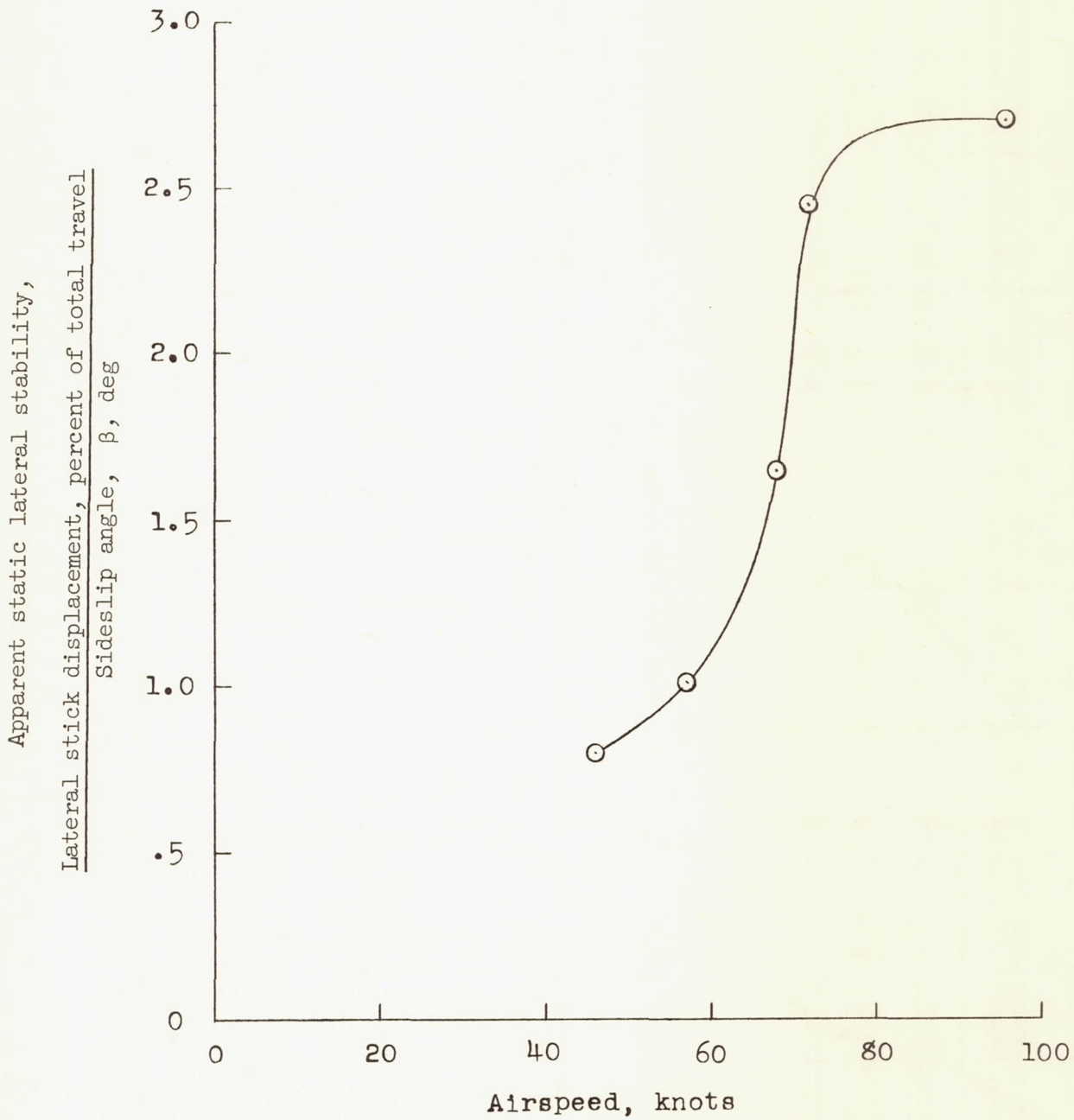

Figure 15.- Variation of apparent static lateral stability with airspeed, level-flight configuration, where airspeed is controlled by duct-angle setting.

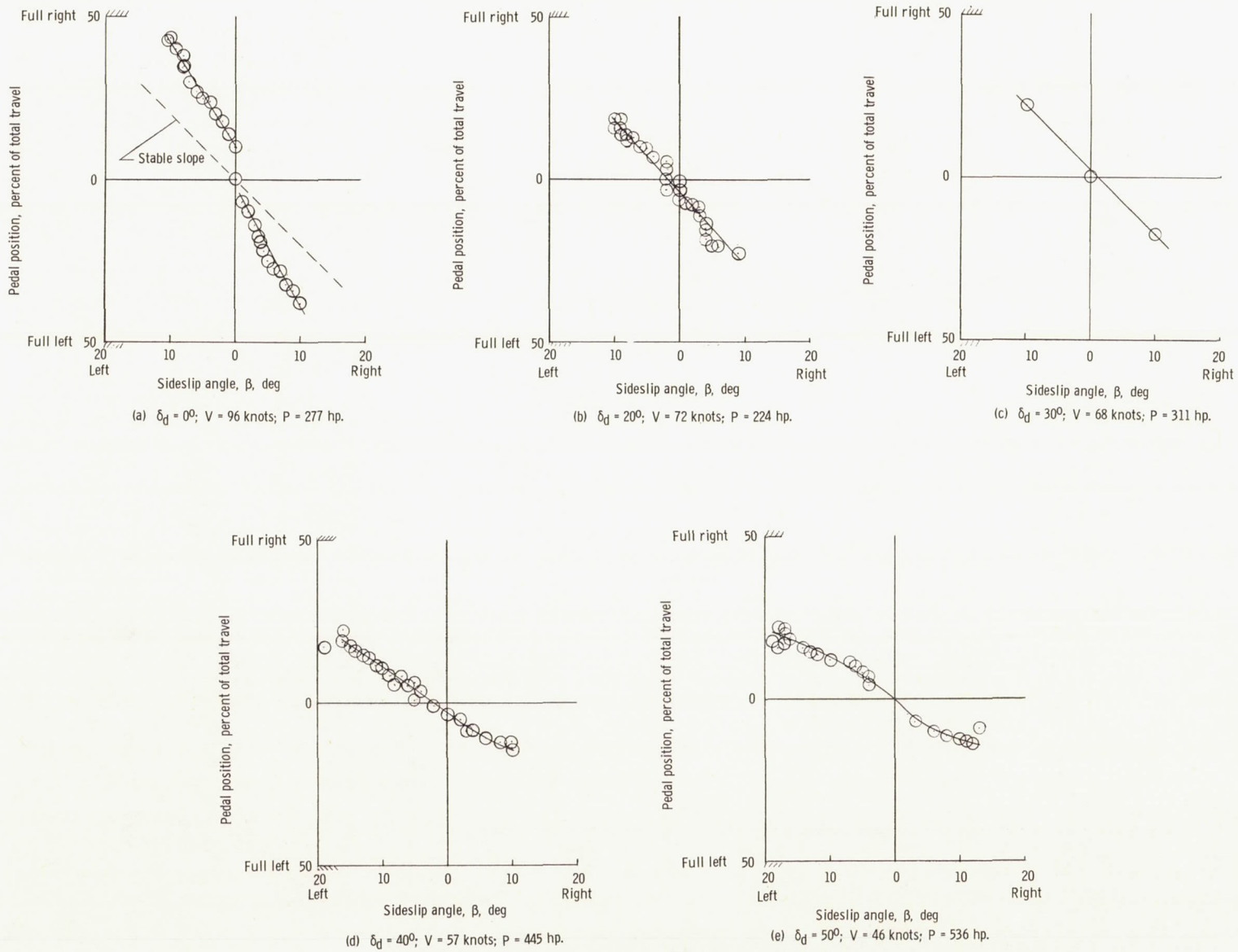

(a) $\delta_d = 0^0$; V = 96 knots; P = 277 hp.

(b) $\delta_d = 20^0$; V = 72 knots; P = 224 hp.

(c) $\delta_d = 30^0$; V = 68 knots; P = 311 hp.

(d) $\delta_d = 40^0$; V = 57 knots; P = 445 hp.

(e) $\delta_d = 50^0$; V = 46 knots; P = 536 hp.

Figure 16.- Static directional stability for several duct angles with the aircraft in level-flight configuration.

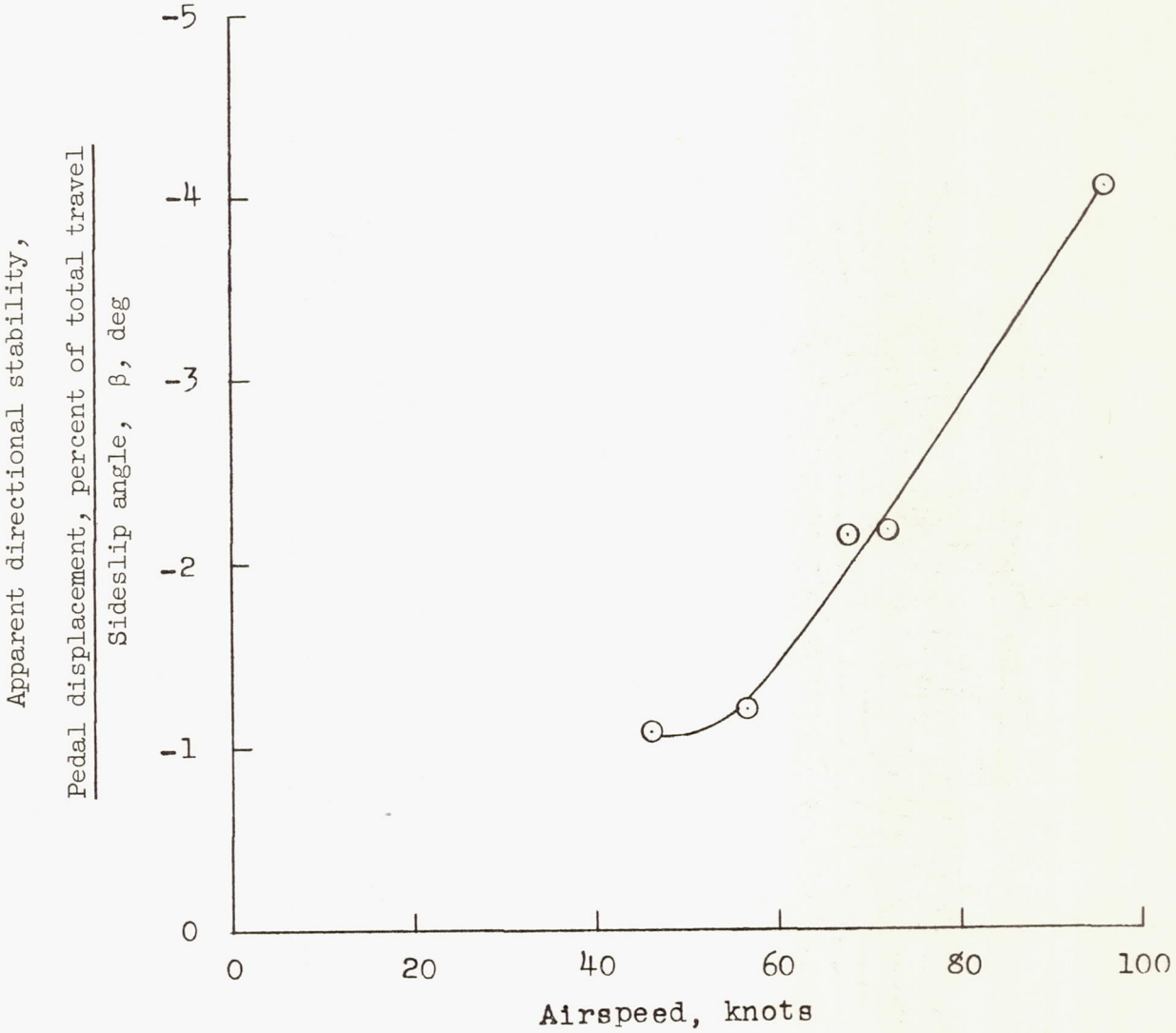

Figure 17.- Variation of apparent static directional stability with airspeed, level-flight configuration, where airspeed is controlled by duct-angle setting.

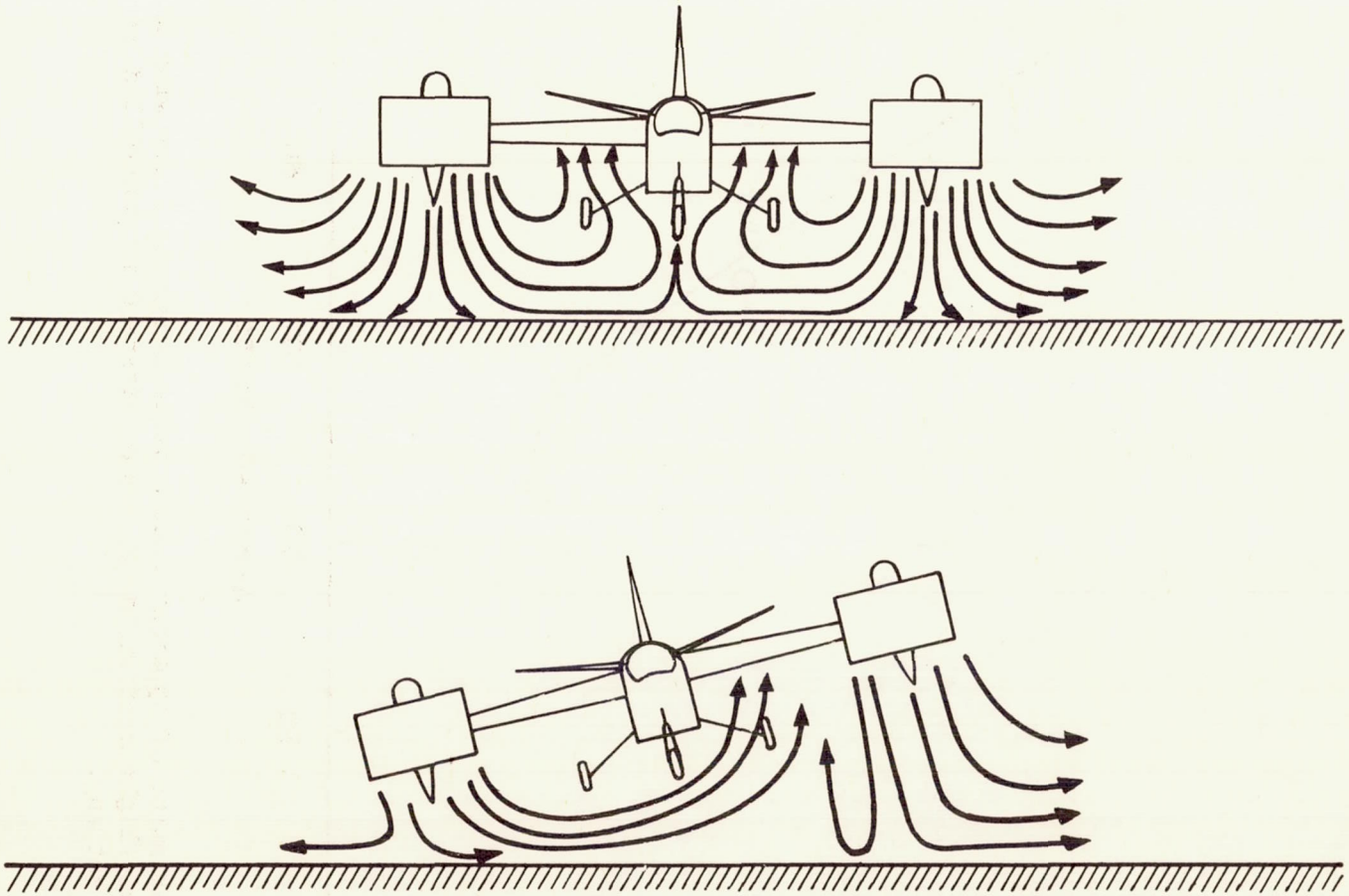

Figure 18.- Typical example of destabilizing effect of downwash from ducted fans as indicated by tufted grids during tethered hovering flight.